

# THE RELEVANCE OF Rb-Sr, Sm-Nd AND Pb-Pb ISOTOPE SYSTEMATICS TO ELUCIDATION OF THE GENESIS AND HISTORY OF RECENT ANDESITE FLOWS AT MT NGAURUHOE, NEW ZEALAND, AND THE IMPLICATIONS FOR RADIOISOTOPIC DATING

ANDREW A. SNELLING, Ph.D.  
INSTITUTE FOR CREATION RESEARCH  
PO BOX 2667  
EL CAJON, CA 92021

## KEYWORDS

Andesite, 1949–1975 flows, Mt Ngauruhoe, New Zealand, Rb-Sr, Sm-Nd, Pb-Pb, radioisotopes, petrogenesis, depleted mantle, magma genesis, crustal contamination, subduction, mixing, inherited radioisotopic ratios, invalid conventional “ages”

## ABSTRACT

Mt Ngauruhoe in the Taupo Volcanic Zone of New Zealand erupted andesite lava flows in 1949 and 1954, and avalanche deposits in 1975. Rb-Sr, Sm-Nd and Pb-Pb radioisotopic analyses of samples of these andesites, as anticipated, did not yield any “age” information, although the Pb isotopic data are strongly linear. When compared with recent andesite flows from the related adjacent Ruapehu volcano, the Sr-Nd-Pb radioisotopic systems plotted on correlation diagrams provide information about the depleted mantle source for the parental basalt magmas and the source of the crustal contamination that produced the andesite lavas from them. The variations in both the depleted mantle Nd “model ages” and the Pb isotopes also suggest radioisotopic heterogeneity in the mantle wedge 80 km below the volcano where partial melting has occurred, contaminated by mixing with trench sediments scraped off the interface with the subducting slab. Thus the radioisotopic ratios in these recent Ngauruhoe andesite flows were inherited, and reflect the origin and history of the mantle and crustal sources from which the magma was generated. By implication, the radioisotopic ratios in ancient lavas throughout the geologic record are likely fundamental to their geochemistry, characteristic of their origin and history rather than necessarily providing valid conventional “ages”.

## INTRODUCTION

With the development of isotope geochemistry in the last 35–40 years has come the realization that radioisotopes may not always provide reliable age measurements. It has been discovered that recent and historic lavas, particularly on oceanic islands, yield incredibly old radioisotopic “ages” [18, 22, 61]. This has led to the recognition that the radioisotopes in these lavas reflect the isotopic compositions of the mantle sources of these lavas, and of any crustal contamination the magmas may have incorporated during ascent and extrusion [18, 22, 59, 61]. The present burgeoning isotope geochemistry literature, reporting increasing numbers of ever more accurate and sophisticated radioisotopic determinations, has only refined the modeling of mantle sources and discussion of their origin, while ignoring the obvious implications for the radioisotopic “age” determinations of ancient lavas being published in the same literature. It was deemed timely, therefore, to undertake an isotope geochemical study of some recent lavas not previously investigated. There were two objectives — to explore the meaning of the radioisotopic ratios in terms of the petrogenesis of the lavas; and thus to recognise the implications for radioisotopic “age” determinations on both recent and ancient lavas.

Chosen for this study was Mt Ngauruhoe, an andesite stratovolcano rising 2291 m above sea level within the Tongariro Volcanic Center of the Taupo Volcanic Zone, North Island, New Zealand (Figure 1) [32, 69]. Though not as well known as its active neighbor, Mt Ruapehu (about 12 km to the south), Ngauruhoe is an imposing, almost perfect cone that rises more than 1000 m above the surrounding landscape. Eruptions from a central 400 m diameter crater have constructed the steep (33°), outer slopes of the cone [41, 69].

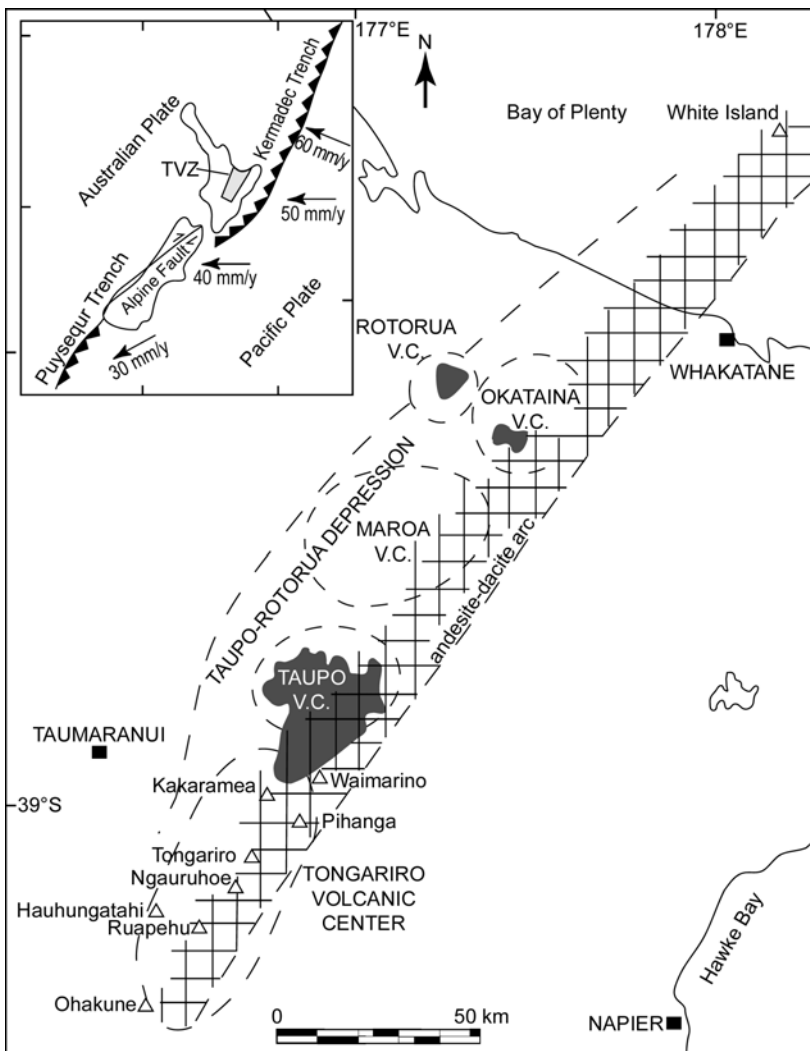


**Figure 1.** The location of Mt Ngauruhoe in the Taupo Volcanic Zone (TVZ), New Zealand, showing the main structural features. The hatched area is the andesite arc, and the solid triangles are basalt-andesite volcanoes. The inset shows the major components of the boundary between the Australian and Pacific Plates in the New Zealand region (arrows indicate relative motions) [32].

Most vents lie close to the axis of a large graben in which Quaternary volcanic rocks overlie a basement of Mesozoic greywacke and Tertiary sediments [38, 56]. North-northeast-trending normal faults with throws up to 30 m cut the volcanoes within the graben. Nearly all vents active within the last 10,000 years lie on a gentle arc which extends 25 km north-northeast from the Rangataua vent on the southern slopes of Ruapehu through Ruapehu summit and north flank vents, Tama Lakes, Ngauruhoe, Red Crater, Blue Lake and Te Mari craters. None of the young vents lie on the mapped faults, which mostly downthrow towards the axis of the graben. The vent lineation lies along this axis, which is considered to mark a major basement fracture [38, 40, 56] that allows the intrusion of andesite dikes.

The Tongariro volcanics unconformably overlie late Miocene marine siltstones beneath Hauhungatahi. A minimum age for the onset of volcanism is indicated by the influx of andesite pebbles in early Pleistocene conglomerates of the Wanganui Basin to the south [12, 40]. Wilson *et al.* [70] suggest a maximum late Pliocene age of 2.0 Ma, based on K-Ar dating of the earliest lavas of the Hauhungaroa cone

## GEOLOGIC SETTING

The Taupo Volcanic Zone is a volcanic arc and marginal basin of the Taupo-Hikurangi arc-trench (subduction) system [9, 10], and is a southward extension on the Tonga-Kermadec arc into the continental crustal environment of New Zealand's North Island. It has been interpreted as oblique subduction of the Pacific Plate beneath the Australian Plate (Figure 1). The zone extends approximately 300 km north-northeast across the North Island from Ohakune to White Island and is up to 50 km wide in the central part, narrowing northwards and southwards. This volcano-tectonic depression (the Taupo-Rotorua Depression [39]) comprises rhyolitic volcanic centers (Rotorua, Okataina, Maroa and Taupo), plus the calc-alkaline Tongariro Volcanic Center. The latter is part of a young (<0.25 Ma) andesite-dacite volcanic arc with no associated rhyolitic volcanism extending along the eastern side of the zone [32].

The Tongariro Volcanic Center extends for 65 km south-southwest from Lake Taupo at the southern end of the Taupo Volcanic Zone (Figure 1), and consists of four large predominantly andesite volcanoes — Kakaramea, Pihanga, Tongariro and Ruapehu (Figure 2); two smaller eroded centers at Maungakatote and Hauhungatahi; a satellite cone and associated flows at Pukeonake; and four craters at Ohakune (Figure 2) [10, 12, 41, 42].

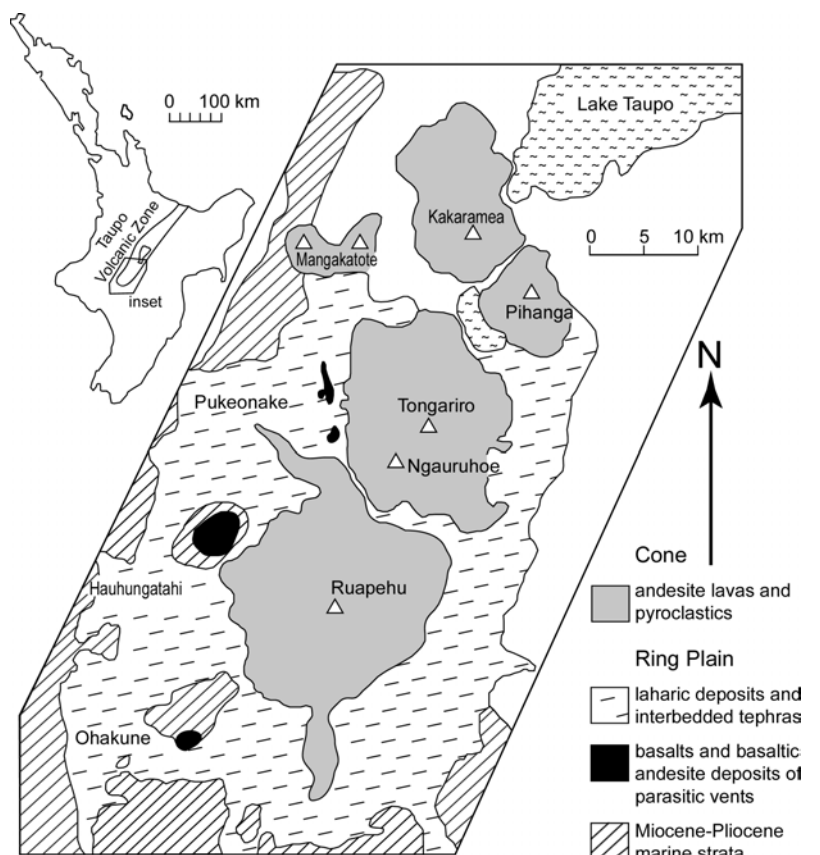


**Figure 2.** Location and deposits of the Tongariro Volcanic Center [12, 41, 42].

[64]. The oldest dated lavas from the Tongariro Volcanic Center are hornblende andesites: exposed at Tama Lakes between Ngauruhoe and Ruapehu, dated at  $0.26 \pm 0.003$  Ma; from Ruapehu, dated at  $0.23 \pm 0.006$  Ma; and from Kakaramea, dated at  $0.22 \pm 0.001$  Ma (all potassium-argon dates) [64].

The Tongariro volcano itself is a large volcanic massif that consists of at least twelve composite cones, the youngest and most active of which is Ngauruhoe. A broad division has been made into older ( $>20$  ka) and younger ( $<20$  ka) lavas [12, 68]. There is a north-northeast alignment of the younger vents of Tongariro, particularly evident between Te Mari and Ngauruhoe.

## NGAURUHOE

Ngauruhoe is the newest cone of the Tongariro Volcanic Center, and has been active for at least 2.5 ka [40, 56, 69]. It has been one of the most active volcanoes in New Zealand, with more than 70 eruptive episodes since 1839, when the first steam eruption was recorded by European settlers [38, 56, 69]. Prior to European colonization the Maoris witnessed many eruptions from the mountain [38]. The first lava eruptions seen by European settlers occurred between April and August 1870, with two or three flows witnessed spilling down the north-western flanks of the volcano on July 7 [38, 56]. Following that event there were pyroclastic (ash) eruptions every few years [56], with major explosive activity in April-May 1948.

The next lava extrusion was in February 1949, beginning suddenly with ejection of incandescent blocks, and a series of hot block and ash flows down the north-western slopes on February 9 [38, 56]. The southern sub-crater filled with lava, which by late on February 10 had flowed over the lowest part of the rim and down the northwest slopes of the cone. By February 12 the flow had ceased. Subsequent mapping placed its volume at about  $575,000 \text{ m}^3$  (Figure 3) [3, 38]. Further explosive pyroclastic (ash) eruptions followed, reaching a maximum about February 19-21. The eruptions ended on March 3.

The eruption from May 13, 1954 to March 10, 1955 began with explosive ejection of ash and blocks. Red-hot lava had been seen in the crater five months previously [38, 56]. The eruption was remarkable for the estimated large volume of almost 8 million  $\text{m}^3$  of lava that then flowed from the crater from June through September 1954, and was claimed to be the largest flow of lava observed in New Zealand (that is, by European settlers) [38, 69]. The lava was actually expelled from the crater in a series of seventeen distinct flows on the following dates [37, 38]:

June 4, 30;

July 8, 9, 10, 11, 13, 14, 23, 28, 29, 30;

August 15(?), 18; and

September 16, 18, 26.

Figure 3 shows the distribution of those 1954 lava flows that are still able to be distinguished on the northwestern and western slopes of Ngauruhoe. All flows were of aa lava (as was the February 11, 1949 flow), typified by rough, jagged, clinkery surfaces made up of blocks of congealed lava. The lava flows were relatively viscous, some being observed at close quarters slowly advancing at a rate of about 20 cm per minute [37, 38, 69]. The August 18 flow was more than 18 m thick and still warm almost a year after being erupted. Intermittent explosive eruptions and spectacular lava fountaining during June and July 1954 built a spatter-and-cinder cone around the south sub-crater, modifying the western summit of the mountain. Activity decreased

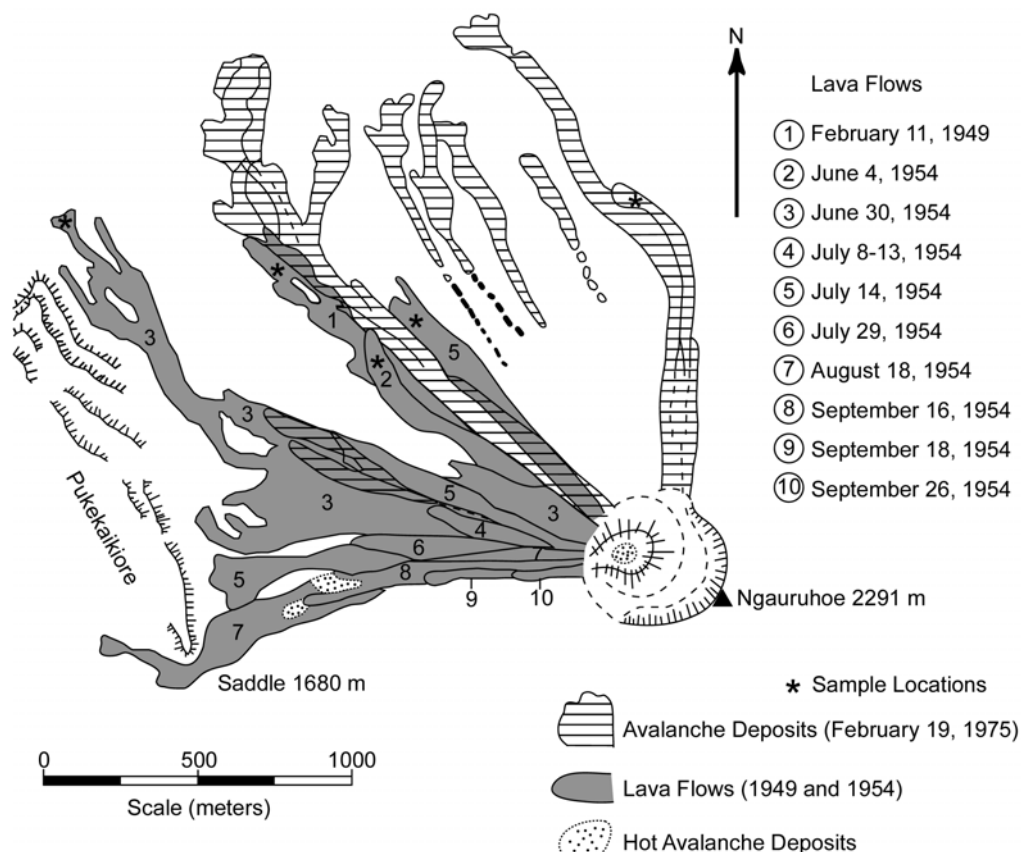


**Figure 3.** Map of the north-western slopes of Mt Ngauruhoe showing the lava flows of 1949 and 1954, and the 1975 avalanche deposits [3, 37, 38, 55, 56]. The location of samples collected for this study are marked.

for two months after the last of the lava flows on September 26, but increased again during December 1954 and January 1955, with lava fountaining and many highly explosive pyroclastic (ash) eruptions. The last ash explosion was reported on March 10, 1955, but red-hot lava remained in the crater until June 1955 [37, 38].

After the 1954-1955 eruption, Ngauruhoe steamed semi-continuously, with numerous small eruptions of ash derived from comminuted vent debris. Incandescent ejecta were seen in January 1973, and ash containing juvenile glassy andesite shards erupted in December 1973 [56]. Canon-like highly explosive eruptions in January and March 1974, the largest since 1954-1955, threw out large quantities of ash and incandescent blocks, one of which was reported as weighing 3000 tonnes and thrown 100 m [56, 69]. Pyroclastic avalanches flowed from the base of large convecting eruption columns, down the west and north slopes of the cone; and the crater became considerably shallower [56, 57].

A series of similar but more violent explosions occurred on February 19, 1975, accompanied by clearly visible atmospheric shock waves and condensation clouds [54, 55, 56, 69]. Ash and blocks up to 30 m across were ejected and scattered within a radius of 3 km from the summit. The series of nine, canon-like, individual eruptions followed a 1.5 hour period of voluminous gas-streaming emission, which formed a convecting eruption plume between 11 km and 13 km high [55, 56, 69]. The explosions took place at 20-60 minute intervals for more than five hours. Numerous pyroclastic avalanches were also generated by fallback from the continuous eruption column. They were a turbulent mixture of ash, bombs and larger blocks which rolled swiftly down Ngauruhoe's sides at about 60 km per hour [56, 69]. The deposits from these avalanches and the later explosions accumulated as sheets of debris in the valley at the base of the cone, but did not extend beyond 2 km from the summit. It is estimated that a minimum bulk volume of 3.4 million m<sup>3</sup> of pyroclastic material was erupted in the seven-hour eruption sequence on that day [55]. Figure 3 shows the location of these avalanche deposits.

There have been no eruptions since February 1975. A plume of steam or gas was often seen above the summit of the volcano for many years, as powerful fumaroles in the bottom of the crater discharged hot gases. The temperature of these fumaroles in the crater floor has steadily cooled since 1979, suggesting that the main vent has become blocked.

### **SAMPLE COLLECTION**

Field work and collection of samples was undertaken in January 1996. The Ngauruhoe area was accessed from State Highway 47 via Mangateopopo Road. From the parking area at the end of the road the Mangateopopo Valley walking trail was followed to the base of the Ngauruhoe cone. From there the darker-colored recent lava flows were clearly visible and easily identifiable against the lighter-colored older portions of the north-western slopes (Figure 3).

Eleven 2–3 kg samples were collected — two each from the February 11, 1949, June 4, 1954 and July 14, 1954 lava flows, and from the February 19, 1975 avalanche deposits; and three from the June 30, 1954 lava flows. The sample locations are marked on Figure 3. Care was taken to ensure correct identification of each lava flow, and that the samples collected were representative of each flow and of any variations in textures and phenocrysts in the lavas.

### **LABORATORY WORK**

All samples were sent first for sectioning — one thin section from each sample. These were subsequently all carefully examined under a petrographic microscope and their mineralogy and textures recorded. A set of representative pieces from each sample (approximately 100 g) was then dispatched to the AMDEL Laboratory in Adelaide, South Australia, for whole-rock major, trace and rare earth element analyses. A representative set (50–100 g from each sample) was also sent to Geochron Laboratories in Cambridge (Boston), Massachusetts, for whole-rock potassium-argon (K-Ar) dating [60]. A third representative set (50–100 g from ten of the samples — two samples from each flow) was sent to the PRISE Laboratory in the Research School of Earth Sciences at the Australian National University in Canberra, Australia, for Rb-Sr, Sm-Nd and Pb-Pb isotopic determinations.

At the AMDEL Laboratory each sample was crushed and pulverized. Whole-rock analyses were undertaken by total fusion of each powdered sample and then digesting them before ICP-OES (inductively coupled plasma — optical emission spectrometry) for major and minor elements, and ICP-MS (inductively coupled plasma — mass spectrometry) for trace and rare earth elements. Fe was analyzed for amongst the major elements by ICP-OES as Fe<sub>2</sub>O<sub>3</sub> and reported accordingly. Additionally, separate analyses for Fe as FeO were undertaken via wet chemistry methods, which were also used to measure the loss on ignition (primarily H<sub>2</sub>O content). The detection limit for all major element oxides was

0.01%. For minor and trace elements the detection limits varied between 0.5 and 20 ppm, and for rare earth elements between 0.5 and 1 ppm.

The Rb-Sr, Sm-Nd and Pb-Pb isotopic analyses were undertaken at the PRISE Laboratory under the direction of Dr Richard Armstrong. No specific sample location or expected age information was supplied to the laboratory, although samples were described as young andesites so that the laboratory staff would optimize the sample preparation procedure in order to obtain the best analytical results. At the laboratory the sample pieces were crushed and pulverized, and then dissolved in concentrated hydrofluoric acid, followed by the standard chemical separation procedures for each of these isotopic systems. Once separated, the elements in each isotopic system were loaded by standard procedures onto metal filaments to be used in the solid source thermal ionization mass spectrometer (TIMS), the state-of-the-art technology in use in this laboratory. Sr isotopes were measured using the mass fractionation correction  $^{86}\text{Sr}/^{88}\text{Sr} = 0.1194$ . The  $^{87}\text{Sr}/^{86}\text{Sr}$  ratios reported were normalized to the NBS standard SRM 987 value of 0.710207. Nd isotopes were corrected for mass fractionation using  $^{146}\text{Nd}/^{144}\text{Nd} = 0.7219$ , and were normalized to the present-day  $^{143}\text{Nd}/^{144}\text{Nd}$  value of 0.51268 for BCR-1. Pb isotope ratios were normalized to NBS standard SRM 981 for mass fractionation.

## PETROGRAPHY AND CHEMISTRY

Clark [6] reported that most of the flows from Ngauruhoe are labradorite-pyroxene andesite with phenocrysts of plagioclase (labradorite), hypersthene and rare augite in a hyalopilitic (needle-like microlites set in a glassy mesostasis) groundmass containing abundant magnetite. However, all lavas, lapilli and incandescent blocks that have been analyzed from eruptions in the twentieth century also contain olivine; so that chemically they may be classed as low-silica (or basaltic) andesites (using the classification scheme of Gill [28]). Previously published analyses [6, 12, 20, 32, 41, 56, 57, 63] show only trivial changes in composition of the lavas and pyroclastics between 1928 and 1975. In fact, the 1954 and 1974 andesites are so similar that Nairn *et al.* [57] suggested that a solid plug of 1954-andesite was heated to incandescence and partially remobilized on top of a rising magma column in 1974. This plug was disrupted and blown from the vent as ejecta ranging in texture from solid blocks, through expanded scoria to spatter bombs.

Table 1 lists the whole-rock major, trace and rare earth element analyses of the eleven samples collected in this study. Comparison of these data for each flow with the corresponding published Ngauruhoe data [6, 7, 11, 12, 20, 32, 41, 63] indicates that in their bulk chemistries all the samples analyzed (and thus all the flows) are virtually identical to one another, the trivial differences, even among the trace and rare earth elements, being attributable to the statistics of analytical errors, sampling and natural variations. Thus it is not unreasonable to conclude that these basaltic andesites are cogenetic, coming from the same magma and magma chamber, even as they have been observed to flow from the same volcano.

Nevertheless, Nairn *et al.* [57] suggested that even though the 1949 and 1954 lavas were both olivine-bearing andesites, analyses of them showed the 1954 lavas to be slightly more basic than the 1949 lava, with slightly higher MgO, CaO and total iron oxides, but lower SiO<sub>2</sub> and alkalis. However, these trends are not duplicated with any statistical significance in the analytical results of this study (Table 1). At least they found that their analyses of the 1974 lava blocks and bombs were identical within the limits of error with the 1954 lavas, which was also substantiated in this study with respect to the 1975 avalanche material and the 1954 lavas (Table 1).

Clark [6] and Cole [7] recognized five lava types in the Tongariro Volcanic Center based on the modal proportions of the phenocryst minerals. Graham [30] modified this scheme to six types based on a combination of mineralogy and chemistry, but given their uniform bulk chemistry and petrology, these Ngauruhoe lava flows group together as plagioclase-pyroxene andesite within Graham's "Type 1". Cole *et al.* [12] have described "Type 1" lavas as volumetrically dominant within the Tongariro Volcanic Center, and as exhibiting coherent chemical trends with increasing silica content. They are relatively Fe-rich and follow a typical calc-alkaline trend on the AFM diagram.

Adapting the terminology of Gill [28], the Ngauruhoe lavas are described as basic andesites (53–58 wt% SiO<sub>2</sub>) [12]. Their designation as plagioclase-pyroxene andesites is based on the predominant phenocrysts present, with plagioclase greater than or equal to pyroxene. The proportion of phenocrysts to groundmass, and the different mineral proportions among the phenocrysts, in the samples collected for this study very closely resemble those in samples reported from the same flows [7, 12].

All samples of the five lava flows examined in this study exhibit a porphyritic texture, with phenocrysts (up to 3 mm across) consistently amounting to 35–40% by volume. The phenocryst assemblage is

| Sample                             | 1A           | 1B     | 2A           | 2B     | 3A            | 3B     | 3C     | 4A            | 4B     | 5A           | 5B     |
|------------------------------------|--------------|--------|--------------|--------|---------------|--------|--------|---------------|--------|--------------|--------|
| Flow Date                          | Feb 11, 1949 |        | June 4, 1954 |        | June 30, 1954 |        |        | July 14, 1954 |        | Feb 19, 1975 |        |
| SiO <sub>2</sub> (%)               | 56.7         | 56.2   | 55.3         | 55.8   | 56.3          | 55.9   | 55.6   | 56.1          | 55.6   | 56.0         | 55.4   |
| TiO <sub>2</sub> (%)               | 0.79         | 0.85   | 0.74         | 0.77   | 0.76          | 0.75   | 0.74   | 0.75          | 0.84   | 0.79         | 0.78   |
| Al <sub>2</sub> O <sub>3</sub> (%) | 17.2         | 17.3   | 16.5         | 17.3   | 17.0          | 16.9   | 16.7   | 16.9          | 17.5   | 17.0         | 16.5   |
| Fe <sub>2</sub> O <sub>3</sub> (%) | 9.10         | 9.63   | 9.26         | 9.23   | 9.11          | 9.17   | 9.59   | 9.29          | 9.61   | 9.25         | 9.43   |
| MgO (%)                            | 4.28         | 3.84   | 5.21         | 4.71   | 4.75          | 5.00   | 5.09   | 4.71          | 3.84   | 4.31         | 5.27   |
| MnO (%)                            | 0.15         | 0.16   | 0.15         | 0.15   | 0.15          | 0.15   | 0.16   | 0.15          | 0.16   | 0.15         | 0.16   |
| CaO (%)                            | 7.61         | 7.93   | 8.22         | 8.29   | 7.95          | 8.16   | 8.17   | 8.00          | 8.17   | 7.83         | 8.56   |
| Na <sub>2</sub> O (%)              | 3.08         | 3.19   | 2.91         | 3.03   | 3.06          | 2.98   | 2.95   | 3.02          | 3.11   | 3.08         | 2.86   |
| K <sub>2</sub> O (%)               | 1.15         | 1.01   | 1.05         | 1.00   | 1.10          | 1.08   | 1.06   | 1.12          | 1.04   | 1.10         | 1.09   |
| P <sub>2</sub> O <sub>5</sub> (%)  | 0.13         | 0.13   | 0.12         | 0.12   | 0.13          | 0.13   | 0.13   | 0.13          | 0.13   | 0.14         | 0.14   |
| LOI (%)                            | 0.42         | 0.48   | 0.51         | 0.37   | 0.38          | 0.50   | 0.53   | 0.62          | 0.42   | 0.70         | 0.41   |
| TOTAL                              | 100.61       | 100.72 | 99.97        | 100.77 | 100.69        | 100.72 | 100.72 | 100.79        | 100.42 | 100.31       | 100.60 |
| Cr (ppm)                           | 60           | 60     | 120          | 80     | 80            | 100    | 100    | 80            | 40     | 60           | 100    |
| Sc (ppm)                           | 25           | 30     | 30           | 30     | 25            | 30     | 30     | 30            | 30     | 30           | 30     |
| V (ppm)                            | 220          | 240    | 220          | 220    | 220           | 220    | 220    | 220           | 260    | 240          | 240    |
| Ni (ppm)                           | 15           | 10     | 31           | 21     | 24            | 29     | 29     | 25            | 7      | 18           | 29     |
| Co (ppm)                           | 20           | 20     | 20           | 20     | 20            | 20     | 20     | 20            | 20     | 20           | 20     |
| Cu (ppm)                           | 180          | 38     | 63           | 57     | 69            | 51     | 69     | 67            | 22     | 51           | 78     |
| Zn (ppm)                           | 87           | 93     | 87           | 84     | 86            | 89     | 85     | 84            | 91     | 88           | 87     |
| Ga (ppm)                           | 24           | 22     | 23           | 28     | 27            | 26     | 26     | 27            | 29     | 27           | 28     |
| Rb (ppm)                           | 36.0         | 26.5   | 29.0         | 32.0   | 32.5          | 30.0   | 29.5   | 35.5          | 32.0   | 31.5         | 31.0   |
| Sr (ppm)                           | 220          | 165    | 200          | 240    | 240           | 240    | 220    | 260           | 260    | 240          | 320    |
| Y (ppm)                            | 19           | 18     | 15           | 19     | 18            | 19     | 18     | 18            | 20     | 19           | 17     |
| Zr (ppm)                           | 100          | 80     | 80           | 80     | 80            | 80     | 80     | 100           | 80     | 100          | 80     |
| Hf (ppm)                           | 10           | 6      | 4            | 4      | 3             | 3      | 3      | 4             | 4      | 3            | 3      |
| Nb (ppm)                           | <10          | <10    | <10          | <10    | <10           | <10    | <10    | <10           | <10    | <10          | <10    |
| Ba (ppm)                           | 200          | 165    | 175          | 185    | 220           | 200    | 200    | 220           | 190    | 200          | 220    |
| Ta (ppm)                           | 3            | 2      | 2            | <2     | <2            | <2     | <2     | 2             | <2     | <2           | <2     |
| Pb (ppm)                           | 20           | 15     | 10           | 10     | 20            | 10     | 10     | 15            | 10     | 15           | 20     |
| Th (ppm)                           | 5.0          | 3.0    | 2.5          | 3.0    | 3.0           | 3.0    | 3.0    | 3.5           | 3.0    | 3.0          | 3.5    |
| U (ppm)                            | 2.0          | 1.5    | 1.0          | 1.0    | 1.0           | 1.0    | 1.0    | 1.5           | 1.5    | 1.0          | 1.0    |
| La (ppm)                           | 12           | 8      | 9            | 11     | 11            | 11     | 11     | 11            | 11     | 11           | 12     |
| Ce (ppm)                           | 25           | 16     | 19           | 22     | 22            | 23     | 22     | 25            | 21     | 22           | 24     |
| Pr (ppm)                           | 4            | 3      | 3            | 3      | 3             | 3      | 3      | 3             | 3      | 3            | 3      |
| Nd (ppm)                           | 18.5         | 14.0   | 10.5         | 12.5   | 12.0          | 13.0   | 13.5   | 14.0          | 14.0   | 11.5         | 14.0   |
| Sm (ppm)                           | 3.5          | 3.0    | 1.5          | 2.5    | 2.5           | 2.5    | 2.5    | 2.5           | 3.0    | 2.5          | 3.0    |
| Eu (ppm)                           | 1.0          | 1.0    | 0.5          | 1.0    | 1.0           | 1.0    | 1.0    | 1.0           | 1.0    | 1.0          | 1.0    |
| Gd (ppm)                           | 3            | 3      | 2            | 3      | 2             | 3      | 3      | 3             | 3      | 3            | 3      |
| Tb (ppm)                           | 0.5          | <0.5   | <0.5         | 0.5    | <0.5          | <0.5   | 0.5    | 0.5           | 0.5    | <0.5         | 0.5    |
| Dy (ppm)                           | 4.0          | 3.5    | 2.5          | 3.5    | 3.0           | 3.5    | 3.0    | 3.5           | 4.0    | 3.0          | 3.5    |
| Ho (ppm)                           | 1.0          | 1.0    | 0.5          | 1.0    | 1.0           | 1.0    | 1.0    | 1.0           | 1.0    | 1.0          | 1.0    |
| Er (ppm)                           | 2            | 2      | 1            | 2      | 2             | 2      | 2      | 2             | 2      | 2            | 2      |
| Tm (ppm)                           | <1           | <1     | <1           | <1     | <1            | <1     | <1     | <1            | <1     | <1           | <1     |
| Yb (ppm)                           | 3            | 2      | 2            | 2      | 2             | 2      | 2      | 2             | 2      | 2            | 2      |
| Lu (ppm)                           | <0.5         | <0.5   | <0.5         | <0.5   | <0.5          | <0.5   | <0.5   | <0.5          | <0.5   | <0.5         | <0.5   |
| K/Rb                               | 319          | 381    | 362          | 313    | 338           | 360    | 359    | 315           | 325    | 349          | 351    |
| Ca/Sr                              | 346          | 481    | 411          | 345    | 331           | 340    | 371    | 308           | 314    | 325          | 268    |

**Table 1.** Whole-rock, major-element oxide, trace element and rare earth element analyses of five recent (1949, 1954, 1975) lava flows at Mt Ngauruhoe, New Zealand (Analyst: AMDEL, Adelaide; April 1996).

dominated (2:1) by plagioclase, but orthopyroxene and augite (clinopyroxene) are always major components, while olivine and magnetite are only present in trace amounts. This POAM (plagioclase-olivine/orthopyroxene-augite-magnetite) phenocryst assemblage is a typical anhydrous mineralogy [12]. The groundmass consists of microlites of plagioclase, orthopyroxene and clinopyroxene, and is crowded with minute granules of magnetite and/or Fe-Ti oxides. Small amounts (9–10%) of brown transparent (acid-residuum) glass are also present, and the overall texture is generally pilotaxitic (the lath-shaped microlites being generally interwoven in an irregular unoriented fashion).

Steiner [63] stressed that xenoliths are a common constituent of the 1954 Ngauruhoe lavas, but also noted that Battey [3] reported the 1949 Ngauruhoe lava was rich in xenoliths. All samples in this study contained xenoliths, including those from the 1975 avalanche material. However, many of these aggregates are more accurately described as glomerocrysts and mafic (gabbro, websterite) nodules [36]. They are 3–5 mm across, generally have hypidiomorphic-granular textures, and consist of plagioclase, orthopyroxene and clinopyroxene in varying proportions, and very occasionally olivine. The true xenoliths are often rounded and invariably consist of fine quartzose material. Steiner [63] also described much larger xenoliths of quartzo-feldspathic composition and relic gneissic structure.

The plagioclase phenocrysts have been recorded as ranging in composition from An<sub>89</sub> to An<sub>40</sub> (andesine to bytownite), but in Ngauruhoe lavas are usually labradorite (An<sub>68-55</sub>). They are subhedral and commonly exhibit complex oscillatory zoning with an overall trend from calcic cores to sodic rims [7, 11, 12]. Thin outer rims are usually compositionally similar to groundmass microlites. Twinning and hourglass structures are common.

Orthopyroxene predominates (>2:1) over clinopyroxene. Subhedral-euhedral orthopyroxene is typically pleochroic and sometimes zoned. Compositions range from Ca<sub>4</sub>Mg<sub>74</sub>Fe<sub>22</sub> to Ca<sub>3</sub>Mg<sub>47</sub>Fe<sub>50</sub> [11, 12], but representative bulk and partial analyses of Ngauruhoe orthopyroxenes [7, 19, 32] indicate a hypersthene composition predominates, which is confirmed by optical determinations [6, 7]. Euhedral-subhedral clinopyroxene is typically twinned and zoned, but compositions show a restricted range of Ca<sub>43</sub>Mg<sub>47</sub>Fe<sub>10</sub> to about Ca<sub>35</sub>Mg<sub>40</sub>Fe<sub>25</sub>, all of which is augite [12, 36].

The olivine present is strongly magnesian, analyses indicating some compositional zoning from Fo<sub>88</sub> to Fo<sub>78</sub>. The magnetite present in the groundmass is titanomagnetite, judging from the amount of TiO<sub>2</sub> present in the whole-rock analyses (Table 1), but some ilmenite is likely to occur sporadically in association with it [12, 36].

As already noted, the trace and rare earth element data in Table 1 indicate that all these samples (and thus all the flows) are virtually identical to one another, the minor differences being attributable to the statistics of analytical errors, sampling and natural variations, and thus are trivial. These data are also comparable to published data [7, 11, 20, 32]. As noted by Graham and Hackett [32], in these “Type 1” or plagioclase-pyroxene andesites Cr and Ni follow a trend similar to that of MgO, so that in samples where the MgO concentration is lower, the Cr and Ni concentrations are also lower, while at the same time the Al<sub>2</sub>O<sub>3</sub> concentration is higher, reflecting less olivine and pyroxene in those samples. The K/Rb ratios vary from 313 to 381 (average 343) and are within the range, and right on the average, of those ratios for plagioclase-pyroxene andesites reported by Cole [7]. Both Rb and Ba are, as expected, positively related to K. Similarly, Sr is positively correlated with Ca, and the Ca/Sr ratios vary from 268 to 481 (average 349), which matches published data [7]. On the other hand, the Zr contents of these lava flows range from 80 to 100 ppm (average 85 ppm), which is less than the published data for plagioclase-pyroxene andesites; whereas the Cu ranges from 22 to 180 ppm, which is higher than the published data.

The normalized geochemical distribution patterns of the trace elements in these lava flows show the characteristic enrichment of large ion lithophile elements (LILE) such as Sr, K, Rb, Ba and Th, and depletion of high field strength elements (HFSE) such as Nb, P, Zr, Ti and Y, in calc-alkaline lavas compared to normal (N-type) mid-ocean ridge basalts (MORB) [32]. The samples from these lava flows also show enrichment of the rare earth elements when compared to chondrite values, and show greater enrichment of the light rare earth elements (LREE) than the heavy rare earth elements (HREE), identical to published data [11]. These plagioclase-pyroxene andesites also all have negative Eu anomalies.

### **K-Ar ISOTOPE SYSTEMATICS**

Snelling [60] reported having obtained K-Ar model “ages” for these same samples of recent Mt Ngauruhoe andesite flows of <0.27 to 3.5 Ma. Such results were expected, as meaningful dates from historic lava flows are not usually obtained, which is recognised in the standard scientific literature [60, 61]. These “dates” could not be reproduced, even from splits of the same samples from the same flow. This apparent inconsistency merely indicates variation in the excess <sup>40</sup>Ar\* (radiogenic <sup>40</sup>Ar) content. Indeed, Ar contamination at such low concentration levels is often expected, but this problem of excess <sup>40</sup>Ar\* in historic lava flows is still well documented in the literature. It was concluded that this excess <sup>40</sup>Ar\* had been inherited by these magmas during their genesis in the upper mantle, and therefore has no age significance.

### **Sr-Nd-Pb ISOTOPE GEOCHEMISTRY**

The results of the Rb-Sr, Sm-Nd and Pb-Pb isotopic analyses are listed in Table 2. The epsilon (ε) values are a measure of the deviations of the isotopic ratios in the samples from the expected value in a uniform reservoir [17]. In Table 2 the epsilon values for both Sr and Nd isotopes have been calculated, comparing the present-day isotopic ratios as measured in these samples with the present-day isotopic ratios of the depleted mantle, the postulated source of the magmas. The positive epsilon values imply that these rocks have greater <sup>87</sup>Sr/<sup>86</sup>Sr and <sup>143</sup>Nd/<sup>144</sup>Nd ratios than those in the depleted mantle source region(s) of the magmas from which they cooled [59]. Calculating the epsilon values for individual samples can be a test of cogenicity or of contamination in the samples, or can be a measure of the extent to which the magmas, when they cooled to form the rocks, had fractionated relative to their

| Sample                               | 1A           | 1B       | 2A           | 2B       | 3A            | 3C       | 4A            | 4B       | 5A           | 5B       |
|--------------------------------------|--------------|----------|--------------|----------|---------------|----------|---------------|----------|--------------|----------|
| Flow Date                            | Feb 11, 1949 |          | June 4, 1954 |          | June 30, 1954 |          | July 14, 1954 |          | Feb 19, 1975 |          |
| Rb (ppm)                             | 36.19        | 45.73    | 36.85        | 104.92   | 37.80         | 24.78    | 69.85         | 50.33    | 55.16        | 36.13    |
| <sup>87</sup> Rb (nm/g)              | 117.94       | 149.01   | 120.08       | 341.88   | 123.18        | 80.74    | 227.62        | 163.99   | 179.73       | 117.74   |
| Sr (ppm)                             | 237.27       | 203.03   | 249.44       | 228.36   | 238.86        | 236.23   | 239.50        | 269.70   | 232.20       | 304.81   |
| <sup>86</sup> Sr (nm/g)              | 267.17       | 228.62   | 280.87       | 257.13   | 268.95        | 266.00   | 269.68        | 303.70   | 261.45       | 343.22   |
| <sup>87</sup> Rb/ <sup>86</sup> Sr   | 0.4414       | 0.65177  | 0.4275       | 1.32962  | 0.4580        | 0.30355  | 0.84405       | 0.5400   | 0.68745      | 0.3431   |
| <sup>87</sup> Sr/ <sup>86</sup> Sr   | 0.70558      | 0.705153 | 0.70552      | 0.705461 | 0.70566       | 0.705401 | 0.705539      | 0.70516  | 0.705599     | 0.70529  |
| $\epsilon_{\text{Sr}}(t_0)$          | +42.41       | +36.34   | +41.56       | +40.72   | +43.55        | +39.87   | +41.83        | +36.47   | +42.68       | +38.29   |
| Sm (ppm)                             | 5.319        | 3.499    | 3.225        | 4.057    | 3.667         | 3.361    | 3.121         | 3.584    | 3.816        | 4.671    |
| <sup>147</sup> Sm (nm/g)             | 5.303        | 3.490    | 3.215        | 4.035    | 3.656         | 3.352    | 3.113         | 3.573    | 3.805        | 4.657    |
| Nd (ppm)                             | 20.886       | 15.640   | 13.660       | 14.256   | 14.912        | 13.968   | 13.258        | 14.515   | 15.742       | 19.350   |
| <sup>144</sup> Nd (nm/g)             | 34.447       | 25.795   | 22.529       | 23.513   | 24.594        | 23.038   | 21.867        | 23.940   | 25.965       | 31.914   |
| <sup>147</sup> Sm/ <sup>144</sup> Nd | 0.15401      | 0.13528  | 0.14276      | 0.17161  | 0.14869       | 0.14550  | 0.14236       | 0.14933  | 0.14655      | 0.14595  |
| <sup>143</sup> Nd/ <sup>144</sup> Nd | 0.512751     | 0.512778 | 0.512731     | 0.512749 | 0.512704      | 0.512720 | 0.512740      | 0.512739 | 0.512742     | 0.512775 |
| $\epsilon_{\text{Nd}}(t_0)$          | +1.38        | +1.91    | +0.99        | +1.35    | +0.47         | +0.78    | +1.17         | +1.15    | +1.21        | +1.85    |
| $T_{\text{DM}}$ (Ma)                 | 1020.4       | 724.5    | 901.7        | 1453.3   | 1047.0        | 962.4    | 877.5         | 974.7    | 927.6        | 845.2    |
| <sup>206</sup> Pb/ <sup>204</sup> Pb | 18.842       | 18.802   | 18.821       | 18.838   | 18.832        | 18.828   | 18.797        | 18.841   | 18.833       | 18.805   |
| <sup>207</sup> Pb/ <sup>204</sup> Pb | 15.635       | 15.631   | 15.629       | 15.632   | 15.632        | 15.636   | 15.629        | 15.637   | 15.630       | 15.620   |
| <sup>208</sup> Pb/ <sup>204</sup> Pb | 38.749       | 38.701   | 38.716       | 38.740   | 38.735        | 38.735   | 38.694        | 38.748   | 38.740       | 38.687   |

- Notes: (1) Measured, present-day <sup>87</sup>Sr/<sup>86</sup>Sr ratios ( $\pm 2\sigma$ ) are normalized to <sup>86</sup>Sr/<sup>88</sup>Sr = 0.1194  
(2) The <sup>87</sup>Sr/<sup>86</sup>Sr ratios are reported relative to a value of 0.710207 $\pm$ 26 ( $\pm 2\sigma$ ) for the NBS standard SRM987 run with these samples  
(3)  $\epsilon_{\text{Sr}}(t_0)$  refers to the present-day, calculated value relative to a depleted mantle <sup>87</sup>Sr/<sup>86</sup>Sr ratio today of 0.7026 [50, 67]  
(4) Measured, present-day <sup>143</sup>Nd/<sup>144</sup>Nd ratios ( $\pm 2\sigma$ ) are normalized to <sup>146</sup>Nd/<sup>144</sup>Nd = 0.7219  
(5)  $\epsilon_{\text{Nd}}(t_0)$  refers to the present-day, calculated value relative to a depleted mantle value of 0.51268 for BCR-1  
(6) Depleted mantle model ages ( $T_{\text{DM}}$ ) calculated using present-day depleted mantle values of <sup>143</sup>Nd/<sup>144</sup>Nd=0.51315 and <sup>147</sup>Sm/<sup>144</sup>Nd=0.2136  
(7) <sup>206</sup>Pb/<sup>204</sup>Pb ratios are normalized to NBS standard SRM981 for mass fractionation, while all other ratios are calculated by a double spiking routine.

**Table 2.** Rb-Sr, Sm-Nd and Pb-Pb isotopic analyses of five recent (1949, 1954, 1975) lava flows at Mt Ngauruhoe, New Zealand (Analyst: Dr R.A. Armstrong, PRISE, Australian National University, Canberra; February 1997-March 2000).

postulated depleted mantle source(s). The  $T_{\text{DM}}$  notation refers to the depleted mantle model ages calculated from the Nd isotope ratios, and is a measure of the length of time each sample has been separated from the mantle from which it was originally derived [59]. It needs to be remembered that the basis of these model age calculations is an assumption about the isotopic composition of the mantle source region from which the magmas that cooled to form these samples were originally derived. Note that the calculated depleted mantle model ages for these recent lava flows range from 724.5 Ma to 1453.3 Ma.

Because these samples are from recent lava flows (only 28–54 years old), the isotope ratios of these samples were not expected to yield any age information. Nevertheless, a thorough analysis of the data was still undertaken to test for any “age” information they might still yield. Selective plotting of the data does yield some seemingly valid isochrons, such as a 5-point Rb-Sr isochron yielding an apparent age of 133 $\pm$ 87 Ma and a 5-point Sm-Nd isochron yielding an apparent age of 197 $\pm$ 160 Ma. The “goodness of fit” statistics for these two isochrons yield low MSWD values of 0.97 and 0.82 respectively (mean square of weighted deviates – a measure of the ratio of observed scatter from the best-fit line to the expected scatter from the assigned errors and error correlations). However, the probabilities of these fits being meaningful are only moderate and the assigned error margins on each of the determined isotopic ratios required to constrain the fits are intolerably large, resulting in final error margins that are more than 50 per cent of the apparent isochron ages. Such selective manipulation of the data is thus not only misleading, but completely meaningless. However, better apparent results are obtainable with the Pb isotopic data, a 7-point isochron yielding a <sup>207</sup>Pb-<sup>206</sup>Pb age of 3908 $\pm$ 390 Ma. The statistics of this fit are much better, with small error margins for each data point and a reasonable MSWD value of 1.07, but the probability of the fit is only moderate and this apparent isochron has intercepts with the Pb isotope growth curve at -92 Ma and 3921 Ma. For comparison, the Pb isotopic data also yield a 9-point <sup>208</sup>Pb-<sup>206</sup>Pb line of best fit with a low MSWD value of 0.45 and a high probability of 0.87. These outcomes would thus seem to have some validity and meaning to them, implying some significance to these trends in the Pb isotopic data.

## DISCUSSION

The andesites of the Taupo Volcanic Zone exhibit compositional characteristics of continental arc lavas worldwide [36], and it is therefore probable that they were generated by similar processes, namely differentiation of mantle-derived basaltic magmas [28]. Petrographic studies of the basalts of the Taupo



Volcanic Zone suggested to Gamble *et al.* [24] that crystal fractionation and accumulation processes could account for much of the diversity observed in their major-element compositions. They concluded that the parental basaltic magmas must be broadly similar to each other, and thus much of the diversity observed in the andesites can be attributed to secondary processes as the magmas ascended through complex plumbing systems in the mantle and crust beneath this volcanic arc. Although primary andesitic magmas have been postulated for some volcanic arcs [1], and some experimental studies indicate that andesitic magmas may be generated from hydrated peridotite in the mantle above subduction zones [48, 53], it is now generally agreed that this mechanism does not explain the origin and formation of the majority of the andesites in the Taupo Volcanic Zone, including these recent andesite flows at Mt Ngauruhoe. Few if any of these andesites have the required attributes (olivine with a composition greater than Fo<sub>90</sub>, high Cr, Ni and Mg, plus low phenocryst contents) to have been derived directly from an andesitic magma generated in the mantle. Cole [7, 8] favored an origin for these Taupo Volcanic Zone andesites from a primary andesitic magma produced by the melting of subducting oceanic crust and assimilated greywacke and other sediments dragged into the mantle with the subducting slab of oceanic crust, but melts from a subducted slab or the lower crust are also unlikely to be of andesitic composition [71].

In one of the earliest investigations of the petrogenesis of these volcanic rocks of the Taupo Volcanic Zone, not only were the lavas and pyroclastics analyzed, but also the Permian to Jurassic interbedded greywackes, siltstones and shales that are spatially related to, and underlie, the volcanics and that were therefore regarded as a potential source of crustal contamination [20, 64]. Using the Sr, Rb, K, U and Th abundances in these rocks and their <sup>87</sup>Sr/<sup>86</sup>Sr ratios, it was concluded that the data were most consistent with the production of the andesites by partial assimilation of sedimentary material by a basaltic magma derived from the upper mantle; the adjacent greywackes, siltstones and shales being the most likely sedimentary material; and the unassimilated gneissic xenoliths probably representing the basement rocks to those sediments. Cole *et al.* [11] found that the rare earth element geochemistry of the andesites suggested the andesite magmas were generated in the upper mantle wedge associated with the subducting slab of the Pacific Plate beneath the Australian Plate (Figure 1, inset), but some crustal contamination also occurred. Indeed, there are several indicators that suggest the andesites have undergone crustal contamination prior to eruption. These include the frequent occurrence of crustal xenoliths [31, 33], elevated and correlated radiogenic and stable isotope ratios [25, 26, 36], and relatively enriched LILE contents, significantly higher than those predicted by crystal fractionation processes alone [11, 32].

Of the possible assimilants, the most likely is the meta-greywacke basement of the Torlesse and/or Waipapa Terranes. Strong correlations between combinations of radiogenic and stable isotopes trend generally towards the compositional fields of these basement rocks, either partly or wholly overlapping with Waipapa compositions [36]. In published models of the postulated assimilation, the more siliceous and radiogenic Torlesse meta-greywacke was preferred to the Waipapa, since a substantially smaller volume was required to satisfy the resultant petrogenesis models [25, 26, 32, 34]. However, although much of the isotopic data for the andesites of the Taupo Volcanic Zone would seem to be explained by binary mixing between primitive basalt magmas and metasedimentary rocks [36], the actual process is undoubtedly more complex. Bulk assimilation is unlikely on thermochemical grounds [4], given the relatively low magmatic temperatures and highly porphyritic nature of the andesites, suggesting that combined assimilation and fractional crystallization (AFC) [16] would have been operating. Thus, as proposed by Graham and Hackett [32], the true assimilant was probably a minimum partial melt of meta-greywacke with higher SiO<sub>2</sub> and LILE than its bulk parent [13], but with similar isotopic composition (assuming equilibrium melting has taken place [44]).

Graham and Hackett [32] and Graham and Cole [34] suggested that Type 1 andesites had been generated from low-alumina basalt, such as a Ruapehu basalt, by AFC (assimilation and fractional crystallization), involving POAM (plagioclase, olivine/orthopyroxene, augite and magnetite [12]) fractionation and assimilation of Torlesse meta-greywacke. Indeed, Graham and Hackett [32] used least squares geochemical modeling to show how the andesite magma from which a 1954 Ngauruhoe lava cooled [63] could have been generated from a parental basalt magma with the composition of a Ruapehu basalt by a process of combined assimilation of crustal material (addition of 6% assimilant) and crystal fractionation (30% removal of crystals). Furthermore, the presence of xenoliths in the Ngauruhoe andesite flows, particularly the vitrified meta-greywacke and gneissic xenoliths, confirm conclusively that the assimilant was most likely a partial melt of gneiss composed of meta-greywacke that was originally a greywacke in the adjacent greywacke-siltstone-shale sediments of the Torlesse Terrane, which outcrops to the east of both Mt Ngauruhoe and Mt Ruapehu, and which is intersected in boreholes under the Taupo Volcanic Zone [29, 32, 36].

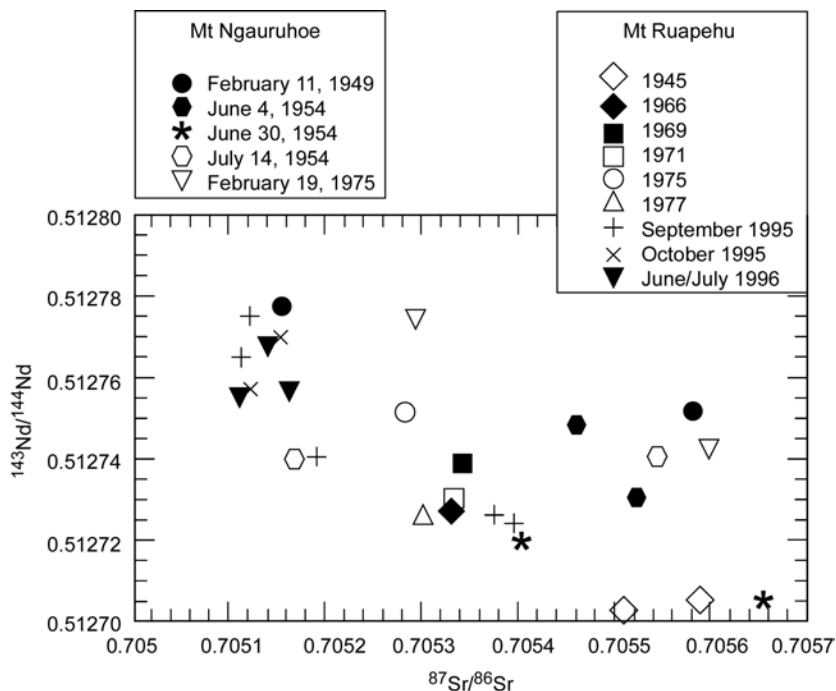


**Figure 4.** Plot of Sr and Nd isotopic compositions of samples of the modern (1945–1996) Ruapehu andesites (after Gamble *et al.* [27]) and the modern (1949, 1954, 1975) Ngauruhoe andesites of this study, showing how similar in isotopic composition these andesites are.

the geochemical data of the Ngauruhoe andesite lavas analyzed for this study with the Ruapehu andesites, it is evident that there are major differences in the major element compositions (for example, the Ruapehu andesites all have higher  $\text{SiO}_2$  contents). However, the  $^{87}\text{Sr}/^{86}\text{Sr}$  and  $^{143}\text{Nd}/^{144}\text{Nd}$  ratios of the recent andesite lava flows from these two adjacent volcanoes are very similar, as can be readily seen in Figure 4. Because it is the Sr-Nd-Pb isotope geochemistry of recent lavas that is used to elucidate their petrogenesis [18, 22, 61], it is not unreasonable therefore to interpret the Sr-Nd-Pb isotope geochemistry of these recent Ngauruhoe andesite lavas in conjunction with the comparable and almost identical isotope data of the closely related recent andesite flows at Ruapehu, and within the framework of the interpreted petrogenesis of the andesites of these two volcanoes.

When plotted on a broader-scale Sr-Nd isotope correlation diagram the recent Ngauruhoe andesite lavas not only plot within the field defined by the recent Ruapehu andesite lavas, but they plot to the right of the mantle array, the band of isotope compositions defined by mid-ocean ridge basalts (MORB) and ocean island basalts (OIB) [49] (Figure 5). Also shown on Figure 5 is the field of Sr and Nd isotopic compositions for the Torlesse greywacke, defined by two metasediment samples and two vitrified metasediment xenoliths [32]. Because the magmas that were extruded as these recent Ngauruhoe and Ruapehu lavas were originally sourced in the mantle, their compositions should have originally been in the field of the mantle array. (These magmas had to be sourced in the mantle because the temperatures in the lower crust are insufficient to generate magmas of a basaltic composition, and because the lower crust is of granitic composition whereas the mantle is basaltic.) Thus whereas these Ngauruhoe and Ruapehu magmas were originally basaltic, by the time of their extrusion they were andesitic in composition. The data plotted on Figure 5 suggest that crustal contamination was responsible for the andesitic composition, and that the Torlesse greywacke has the isotopic composition consistent with the shift in the magmas' compositions away from the mantle

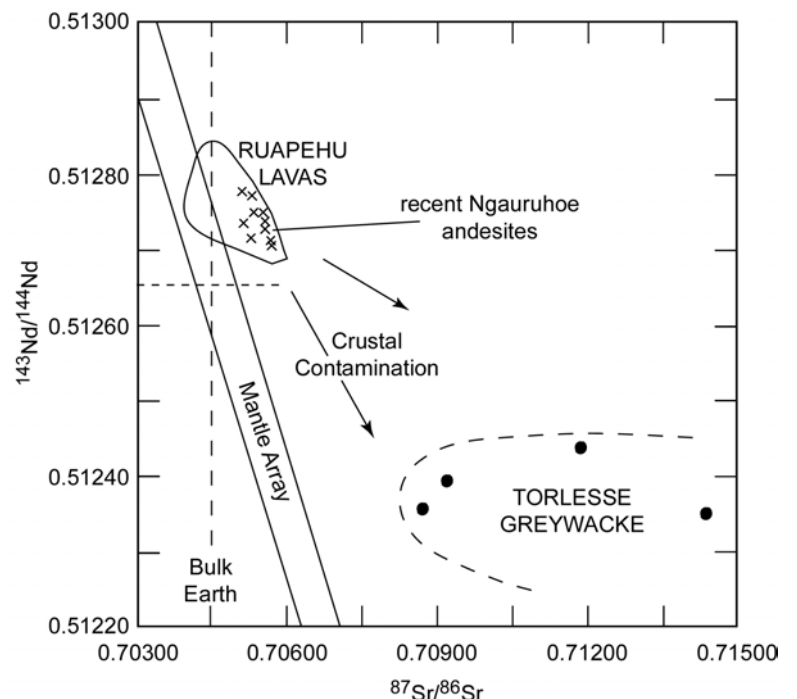


**Figure 5.** Sr-Nd isotope correlation diagram showing the Sr and Nd isotopic compositions of the recent Ngauruhoe lavas, which plot within the compositional field of the spatially and genetically related Ruapehu andesite lavas. The mantle array is defined by MORB and OIB [49]. The field of the Torlesse greywacke is defined by two metasediment samples and two vitrified metasediment xenoliths [32].

Given the close proximity of Ngauruhoe and Ruapehu to one another as adjacent volcanoes developed from related vents in the Tongariro Volcanic Center [12, 32, 42], it would be expected that recent andesite lava flows from these two volcanoes could well have been generated from the same source in a similar manner. Gamble *et al.* [27] have compiled and reviewed the available geochemical and isotopic data for andesite lava flows between 1945 and 1996 from the Ruapehu volcano, and concluded that collectively the data show trends with time of increasing  $\text{SiO}_2$  abundance and rising  $^{87}\text{Sr}/^{86}\text{Sr}$  ratios. This is consistent with broad control of the magma chemistry, and thus the resultant andesite lavas, by assimilation and crystal fractionation (AFC) processes. Furthermore, they found that the magmas emplaced at Ruapehu during that 50 year period show geochemical variability that spans most of the range shown by lavas erupted over the entire history of the volcano. In comparing

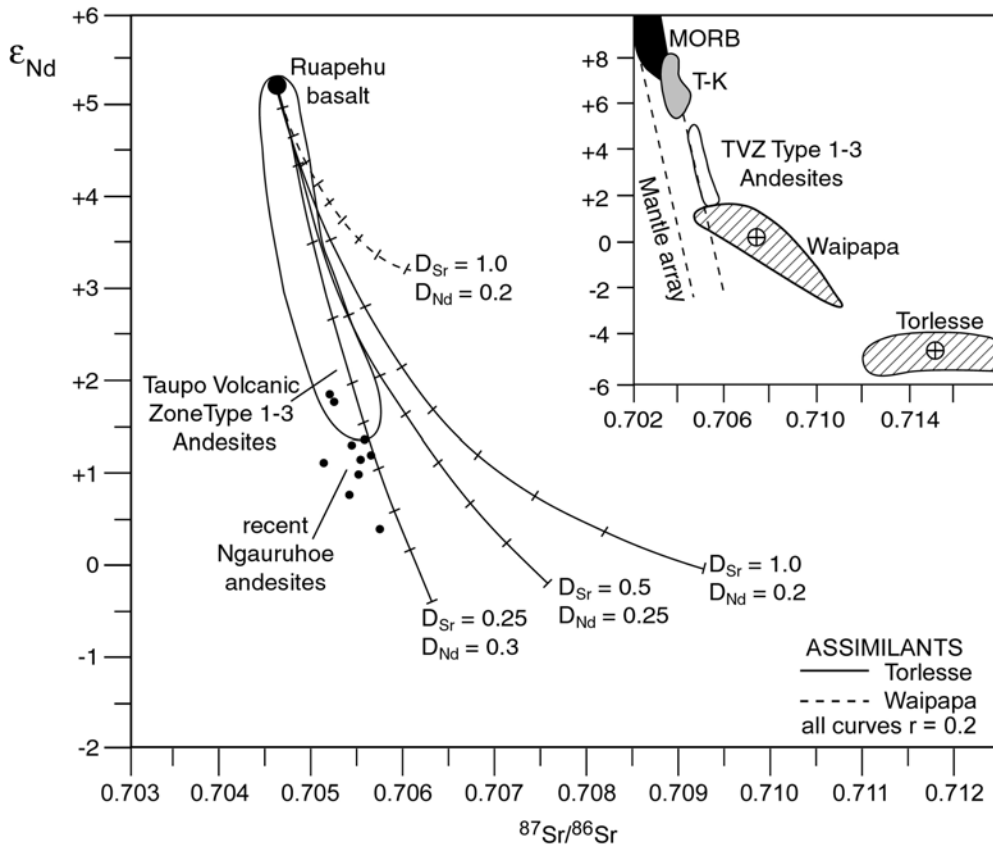


**Figure 6.** An  $^{87}\text{Sr}/^{86}\text{Sr}$  versus  $\epsilon_{\text{Nd}}$  diagram showing where the Ngauruhoe andesites in this study plot in relation to the field of compositions for Taupo Volcanic Zone Type 1–3 andesites [35]. The representative AFC curves are for various combinations of the postulated Ruapehu basalt parent magma [36], assimilant and bulk distribution coefficients ( $D_{\text{Sr}}$ ,  $D_{\text{Nd}}$ ). Tick marks indicate the degree of crystallization and are given in intervals of 0.1 to a maximum of 0.9. In the inset the T-K field represents the lavas of the Tonga-Kermadec Arc.

Volcanic Zone Type 1–3 andesites [36]. The majority of these Ngauruhoe Type 1 andesite lavas plot outside this field and would seem comparable to the Taupo Volcanic Zone rhyolites that plot in the same area [36], perhaps suggesting an even greater degree of fractional crystallization than the other andesites. The representative AFC (assimilation and fractional crystallization) curves were constructed (after DePaolo [16]) for various combinations of a parental Ruapehu basalt, Torlesse and Waipapa assimilants, and bulk distribution coefficients ( $D_{\text{Sr}}$ ,  $D_{\text{Nd}}$ ). It is immediately evident that the AFC mixing curve for a nominal average Waipapa Terrane meta-greywacke is tangential well to the right of, and for >90% crystallization falls well short of, the Type 1–3 andesites field; and the Ngauruhoe andesites in particular. In contrast, the low-alumina Ruapehu basalt–Torlesse Terrane meta-greywacke AFC curves lie within and to the right of the Type 1–3 andesites field, so any substantial Waipapa component would push them further to the right. This would thus appear to rule out any Waipapa component. The curve best matching the trend in the recent Ngauruhoe andesites data does closely match one of these Ruapehu basalt–Torlesse AFC curves, with the degree of crystallization required to explain the isotope shifts being between 40 and 70%. Although this  $^{87}\text{Sr}/^{86}\text{Sr}$  versus  $\epsilon_{\text{Nd}}$  trend could be interpreted as due to source-related processes, as suggested in the Aleutian Arc [49], Graham *et al.* [36] found that this could not be true for the  $\delta^{18}\text{O}$  versus  $^{87}\text{Sr}/^{86}\text{Sr}$  trend for the Taupo Volcanic Zone Type 1–3 andesites, where the initially sharp increase in  $\delta^{18}\text{O}$  with respect to  $^{87}\text{Sr}/^{86}\text{Sr}$  is unmistakably due to crustal assimilation [47, 66]. A similar explanation is evident for the andesite of the Lesser Antilles Arc [14].

The inset to Figure 6 shows the broader isotopic context of these recent Ngauruhoe andesites. Whereas the volcanics of the Tonga-Kermadec Arc [21] were generated from a mantle source less depleted than mid-ocean ridge basalts (MORB) [46], it would appear that the parent basaltic magmas to the Taupo Volcanic Zone Type 1–3 andesites were derived from an even less depleted mantle source. Furthermore, the increase in  $^{87}\text{Sr}/^{86}\text{Sr}$  that shifts both the Tonga-Kermadec lavas and the Taupo Volcanic Zone andesites out of the mantle array [58] is indicative of crustal contamination/assimilation, as are the high positive  $\epsilon_{\text{Sr}}$  values for the recent Ngauruhoe andesites (Table 2), although a portion of these large positive values could also indicate a high degree of fractionation of the magmas relative to their postulated depleted mantle source. Nevertheless, the extreme Sr and Nd isotopic enrichment of the Torlesse assimilant, demonstrated to be the most likely crustal contaminant in these andesites, underlines how only a small proportion of this contaminant (postulated at around 6% [32]) is required.

Plots of the Pb isotope data also graphically illustrate these trends (Figure 7). Gamble *et al.* [27] found

array due to that crustal contamination. Graham and Hackett [32] found that within the broad field in which the recent Ruapehua lavas plot, to the right away from the mantle array, there is a trend in the Type 1 lavas from basalt through andesite to dacite of increasing  $^{87}\text{Sr}/^{86}\text{Sr}$  and decreasing  $^{143}\text{Nd}/^{144}\text{Nd}$ . Similar trends in volcanic rocks in other locations have been similarly explained in terms of crustal assimilation [23]. These data, including the recent Ngauruhoe andesites, are consistent with the classification by Nohda [58] of the Taupo Volcanic Zone as a continental island arc.

This contamination trend that explains the andesite compositions is more pronounced, and therefore graphically illustrated, in the  $^{87}\text{Sr}/^{86}\text{Sr}$  versus  $\epsilon_{\text{Nd}}$  diagram of Figure 6. The recent Ngauruhoe andesites plot within and beyond the field defined by other Taupo

no systematic variation with time in the Pb isotopic data from the recent Ruapehu andesites, while samples from the 1995-1996 Ruapehu lavas yielded  $^{206}\text{Pb}/^{204}\text{Pb}$  ratios which spanned the entire range of compositions from the previous 50 years. Nevertheless, the modern andesitic lavas were less radiogenic than the majority of prehistoric Ruapehu andesites and Taupo Volcanic Zone basalts, with all samples defining a potential mixing array towards the Torlesse Terrane meta-greywacke basement, the major upper crustal component in the region and thus the putative crustal contaminant for most Taupo Volcanic Zone magmas [26, 36, 51]. Furthermore, the Pb isotope data would suggest that the Taupo Volcanic Zone basalts were derived from a depleted mantle source that was more radiogenic than that from which the Pacific MORB was generated. Because the parent basalt magmas that were contaminated to form the andesite lavas were probably from identical depleted mantle sources as the magmas that produced the Taupo Volcanic Zone basalts, the less radiogenic portion of the andesite fields in Figure 7 suggest that the sources for all the parental basalt magmas were much closer to the composition of the depleted mantle sources for the Pacific MORB, while the parental magmas for the Taupo Volcanic Zone basalts must have thus suffered from some crustal contamination similar to the andesites, as suggested by the Sr-Nd isotopic data [36].

As already noted, the Pb isotopic data for the recent Ngauruhoe andesite lavas are strongly linear, particularly the  $^{208}\text{Pb}/^{206}\text{Pb}$  data. The  $^{207}\text{Pb}/^{206}\text{Pb}$  data yield an apparent 7-point isochron with a  $3908 \pm 390$  Ma “age”. Not only is this “age” somewhat meaningless based on the statistics of the fit; these data lie to the right of the geochron, the Pb isochron corresponding to the presumed age of the earth [18, 59, 61]. This is the “lead paradox”, which implies that the depleted mantle has an average composition more radiogenic than the geochron. This is the opposite of the postulated behavior expected in conventional radiogenic isotope geology. Nevertheless, these linear arrays in the recent Ngauruhoe andesite data not only imply Pb isotopic mixing of the assimilated Torlesse contaminant with the parental basalt magmas, but also mixing of leads of differing isotopic compositions in the depleted mantle source of these magmas [18, 22]. It would also seem highly significant that the linear arrays of the recent Ngauruhoe andesite Pb-isotopic data parallel the Pb isotopic compositional field for the Taupo Volcanic Zone basalts, as well as being parallel to the Northern Hemisphere Reference Line (NHRL) [43] and sub-parallel to the compositional field of Pacific MORB [46]. Indeed, this would appear to imply that much of the Pb isotopic variation in both the recent Ngauruhoe andesites and the Taupo Volcanic Zone basalts is probably due to Pb isotopic variations in the depleted mantle source region for the parental basalt magmas. Superimposed on this mantle source Pb-isotopic variation is the Torlesse basement contamination. This would explain the shift in the Ngauruhoe andesite linear arrays upwards toward the Pb isotopic compositional field for the Torlesse basement while still parallel to the Pb-isotopic compositional field of the Taupo Volcanic Zone basalts that are supposed to be similar to the compositions

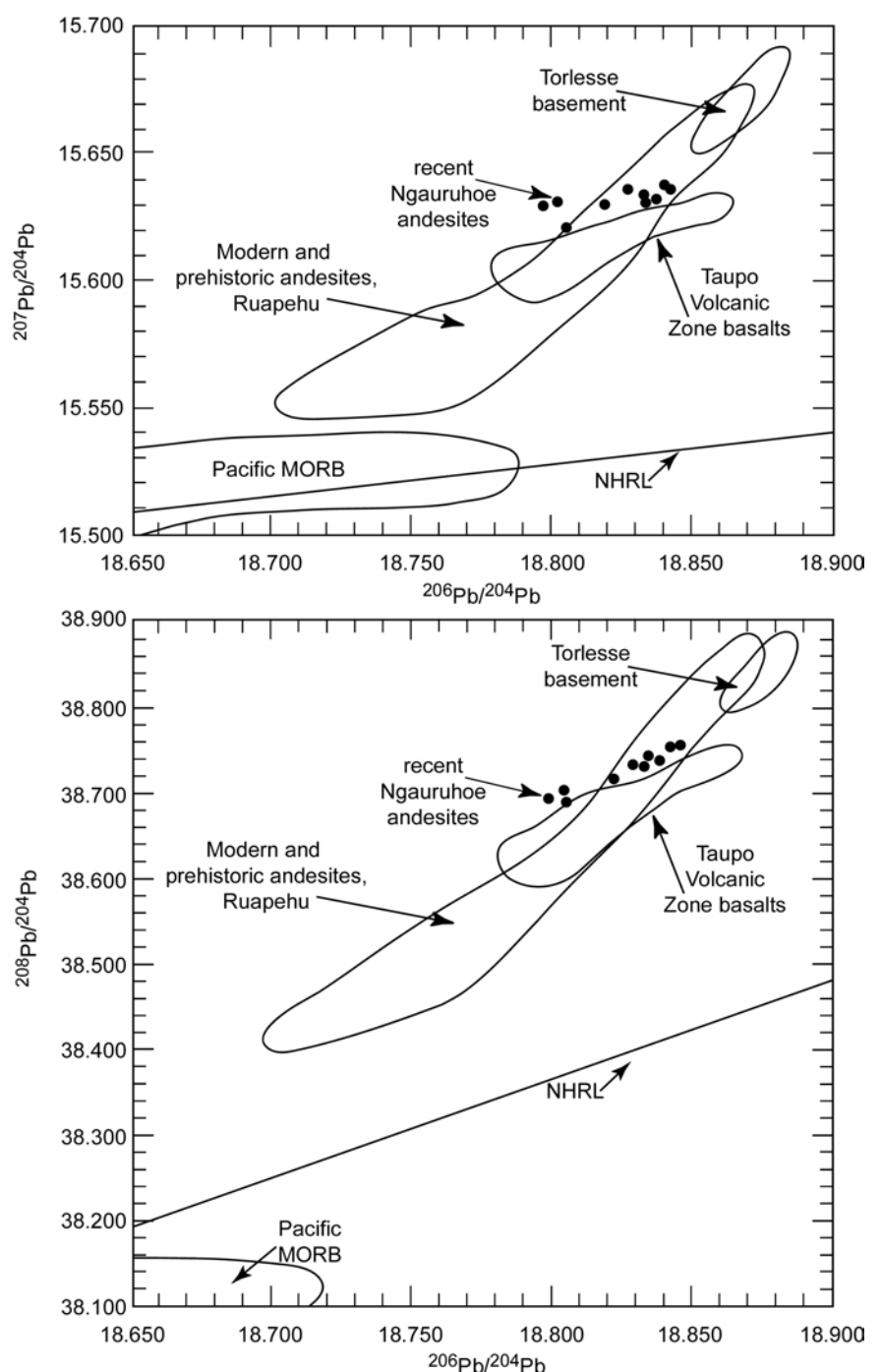


**Figure 7.**  $^{207}\text{Pb}/^{204}\text{Pb}$  and  $^{208}\text{Pb}/^{204}\text{Pb}$  versus  $^{206}\text{Pb}/^{204}\text{Pb}$  plots for modern (1945–1966) and prehistoric Ruapehu andesites [27], Taupo Volcanic Zone basalts [26, 36] and recent Ngauruhoe andesites (this study). The Pb isotopic data suggest contamination of a Pacific MORB source [46] with the Torlesse basement metasediments [35, 51]. NHRL is the Northern Hemisphere Reference Line [43].

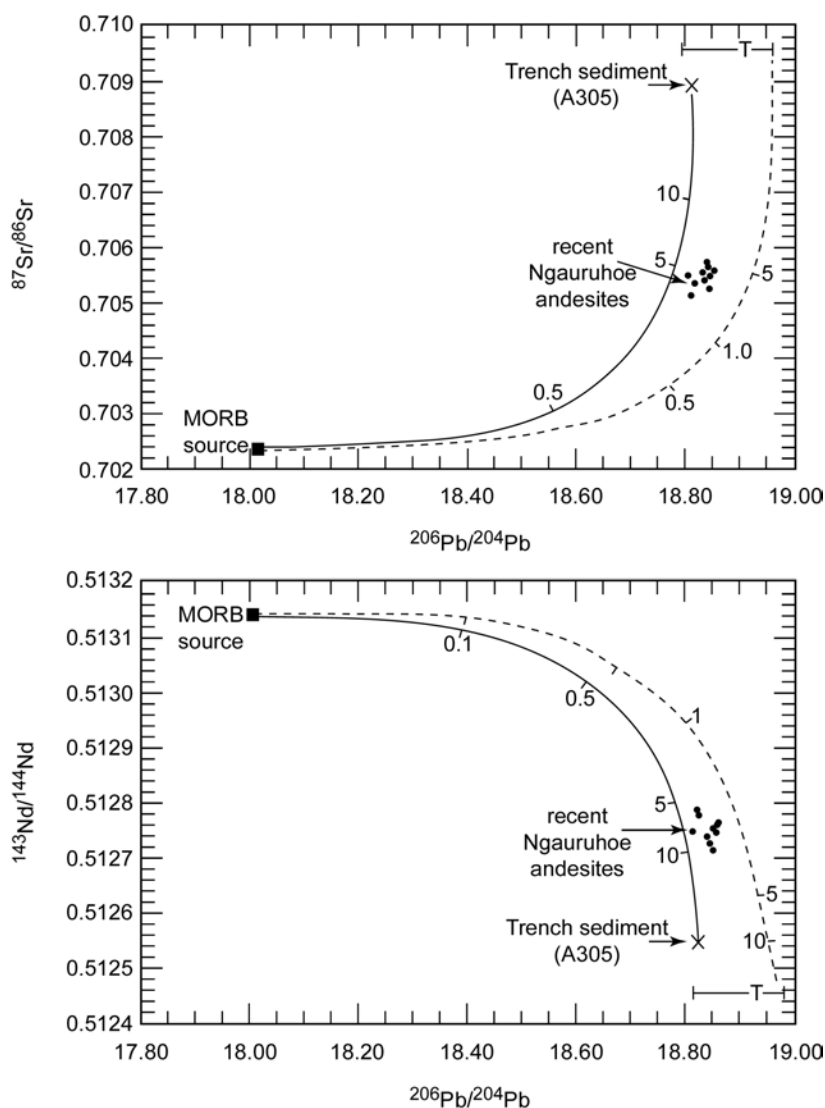


**Figure 8.** Plots of  $^{87}\text{Sr}/^{86}\text{Sr}$  and  $^{143}\text{Nd}/^{144}\text{Nd}$  versus  $^{206}\text{Pb}/^{204}\text{Pb}$  for the recent Ngauruhoe andesites. Calculated bulk mixing curves for MORB–sediment A305 (continuous line) and MORB–Torlesse basement (dashed line) are shown [26]. T is the average composition of the Torlesse metasediments and the horizontal bar delineates the range of their compositions [35]. Tick marks are percent of sediment added to the MORB-source end-member.

displaying many features typical of subduction zone magmas. Figure 8 also has plotted on it the Sr-Pb and Nd-Pb data for the recent Ngauruhoe andesites, which sit between the calculated bulk mixing curves for MORB–trench sediment and MORB–Torlesse basement, as do most of the basaltic samples in the Gamble *et al.* [26] study. Note that the overall range of isotopic compositions for the Torlesse metasediments [35] spans the range of isotopic compositions between these two bulk mixing curves, so it can be reasonably concluded that the recent Ngauruhoe andesite lavas resulted from the contamination of a basaltic magma from a MORB-source with around 5% Torlesse basement metasediment. Thus the Gamble *et al.* [26] study confirms the conclusions reached previously by Graham and Hackett [32].

However, whereas Graham and Hackett [32] regarded this crustal contamination as being the secondary process of crustal assimilation whereby magma compositions are influenced *en route* to the surface through the crust, Gamble *et al.* [26] concluded that the crustal contamination was due to the source-modifying process of sediment subduction into the mantle. The two processes are fundamentally different. However, in the continental New Zealand situation, as a result of the oblique plate convergence and rapid uplift, the sediments which are being subducted offshore in the Hikurangi Trough are essentially the same as the crust made up of Torlesse metasediment basement which is available for assimilation [51]. From modeling based upon Sr and Nd isotope data, Gamble *et al.* [35] had concluded that small amounts of crustal assimilation (up to 10%) could account for the compositions of the basalts in the Taupo Volcanic Zone. However, Gamble *et al.* [26] conclusively demonstrated, from isotope and multi-element variations with latitude in the volcanics and ocean-floor sediments, that the amounts of sediments which contributed to the sources of the arc magmas had a diminishing continental contribution from ~5% in the south (Hikurangi Trough) to <1% in the north (Kermadec Trench). This is consistent also with currently available seismic and sediment dispersion data along the Kermadec-Hikurangi Margin. These data indicate northward thinning of the trench fill deposits [5]. Furthermore, since there is

of the basalt magmas parental to these recent Ngauruhoe andesites.

Using trace elements and their ratios, Gamble *et al.* [25] reviewed the question of source heterogeneity and fertility of the basalt magmas of the Taupo-Kermadec Volcanic Arc systems, and concluded that magma sources were MORB-like, as is also suggested by the Sr-Nd-Pb isotopic data. Thus, using combinations of a MORB-source with typical Kermadec Trench-Hikurangi Trough sediments and with Torlesse metasediments, Gamble *et al.* [26] undertook mixing calculations based on isotope pairs such as  $^{206}\text{Pb}/^{204}\text{Pb}$  versus  $^{143}\text{Nd}/^{144}\text{Nd}$  and  $^{87}\text{Sr}/^{86}\text{Sr}$  (Figure 8). It was thus found that the incorporation of a relatively small amount (up to ~5%) of New Zealand continental sediment (~20 ppm Pb, ~2-3 ppm U and ~14 ppm Th — the average New Zealand Torlesse metasediment of Graham *et al.* [35]) to basalt magmas from a MORB-source could have brought about massive shifts in the isotopic compositions of the resulting basalts of the Kermadec-Taupo Arc, the sediment-hosted Pb having a swamping affect on the “mantle Pb”. Indeed, these bulk mixing calculations showed that mixing <5% of a trench sediment, with a composition such as that of sample A305, with MORB mantle embraced the entire Sr, Nd and Pb isotope data array of the Kermadec-Taupo Arc magmas (Figure 8). Similar calculations based on trace elements produced multi-element diagrams that mimicked multi-element diagrams for the arc basalts,

no continental crust as basement to the Kermadec Island Arc, the crustal contamination there of <1%, derived from the bulk mixing curves on the Sr-Pb and Nd-Pb plots (Figure 8), had to be contributed by subduction of the trench sediments. Thus it can be concluded that the ~5% crustal contamination in the Taupo Volcanic Zone lavas, including the recent Ngauruhoe andesites, was similarly contributed by subduction of the thicker sediments in the Hikurangi Trough to the east of the Taupo Volcanic Zone.

The petrogenetic model favored by Gamble *et al.* [26], which is consistent with all the isotopic data discussed, is shown in Figure 9, based on Tatsumi [65] and Davies and Stevenson [15]. This model envisages a zone of melt formation approximately coincident to the volcanic front, which includes Ruapehu and Ngauruhoe, and a melt generation region delimited by the interface of the subducting slab, the base of the arc lithosphere (of continental New Zealand) and two vertical columns, one delineating the volcanic front, the other, the coupled back-arc basin. Fluids liberated from the descending slab ascend into and enrich the overlying peridotitic mantle wedge. In the region immediately adjacent to the slab mineral reactions would probably have stabilized amphibole. Sediment scraped from the upper surface of the slab is incorporated into the mantle wedge along the slab-mantle interface. Mantle flow

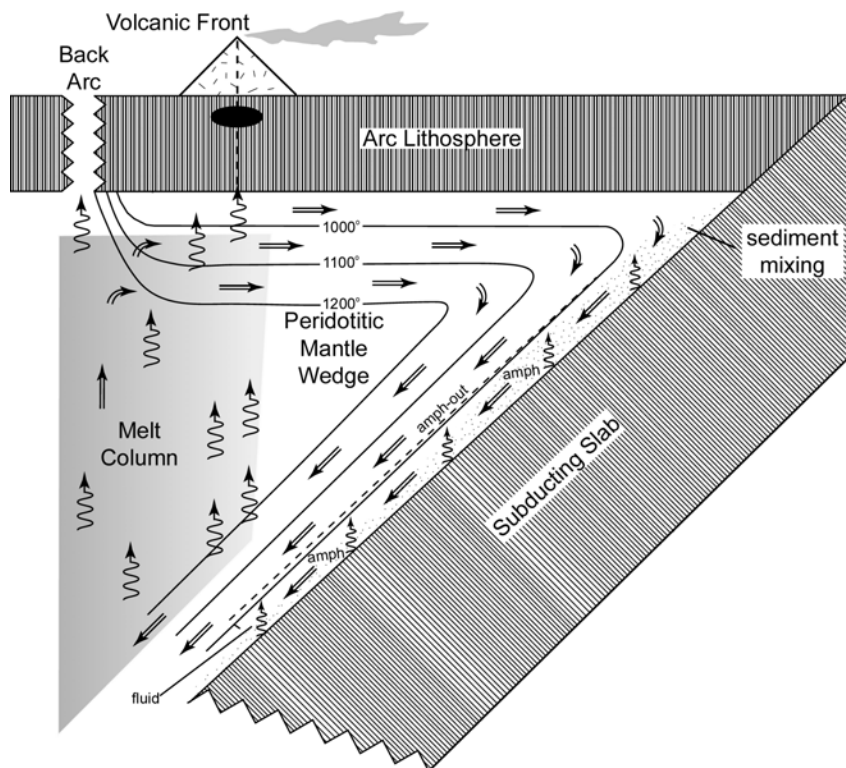


**Figure 9.** Dynamic petrogenetic model for andesite magma genesis beneath the Kermadec-Taupo Volcanic Arc subduction system [15, 26, 65]. Flow lines (arrows with double lines) show mantle flowing from the back-arc region into the mantle wedge, where the isotherms are inverted owing to the cooling effect of the cold subducting “Cretaceous” slab [52]. Sediment that was deposited on the oceanic crust and thus also subducted is mixed into the wedge assemblage along the interface. Progressive dehydration reactions in the slab lead to fluid transfer from the slab into the mantle wedge. In the juxtaposed wedge, amphibole (amph) is stabilized, but then breaks down over the depth range  $112 \pm 19$  km [65], inducing partial melting. In the resulting melt column, the first formed melts accumulating closest to the slab-mantle interface will be most susceptible to fluxing from the slab. Above this zone, melting will continue. The rising melts will eventually pool in the melt column, and the resulting magma finally ascends into the overlying arc lithosphere along fracture conduits, filling magma chambers and triggering eruptions.

parallel to the slab-wedge interface carries the amphibole peridotite down to higher pressures. There the amphibole breaks down, giving rise to amphibole dehydration, while progressive dehydration reactions in the slab itself lead to fluid transfer from the slab into the mantle wedge. Both processes produce partial melting as amphibole breaks down over the depth range  $112 \pm 19$  km [15, 26]. The lower density melt then rises and pools in the upwelling melt column, eventually penetrating upwards into the overlying arc lithosphere to fill magma chambers that then erupt when full.

It is abundantly clear, therefore, from the foregoing discussion and the isotopic data yielded by these recent Ngauruhoe andesite flows, that no “age” information is provided by the Rb-Sr, Sm-Nd and Pb-Pb radioisotopic systems. This is even true of the calculated depleted-mantle Nd model ages, which range from 724.5 Ma to 1453.3 Ma. By definition these model ages are a measure of the length of time each sample has been separated from the mantle from which it was originally derived [59]. But all the evidence is consistent with the magmas responsible for these recent lava flows having formed only recently from partial melting of the mantle wedge beneath the volcano. The subduction of the Pacific Plate beneath New Zealand only began recently, even in conventional terms, because the subducting slab is regarded in conventional terms as Cretaceous [52]. Even the Torlesse metasediments that underlie the Taupo Volcanic Zone and are adjacent to it yield a Rb-Sr whole-rock isochron “age” of only  $141 \pm 3$  Ma [29]. This is interpreted to represent the timing of low-grade metamorphism of these sediments which are regarded in conventional terms to be of Permian to Jurassic age (between 290 and 142 Ma). However, these Nd model ages are a product of the Sm-Nd radioisotopic system within the mantle wedge that has been partially melted near the interface with the subducting slab. Since the subduction is only recent, the melt that separated was formed only recently. Thus these Nd isotopic signatures have been inherited from the partial melting of the mantle wedge, which of course has not occurred over a period of 400–500 million years, as these Nd model ages (Table 2) would otherwise imply. Therefore the Nd isotopes, as the Sr and Pb isotopes, have only been used to elucidate the genesis and history of these recent

Ngauruhoe andesite flows. The radioisotopic ratios are characteristic of the heterogeneity in the mantle source of the magmas, and of the crustal contamination assimilated in the original basaltic magmas. These conclusions support the contention of Snelling [61] that the radioisotopes in these lava flows are an artifact of the mixing of mantle and crustal sources; and that the radioisotopic ratios, which could be interpreted in terms of millions of years of radioactive decay, are instead geochemical characteristics of the mantle and crustal rocks that were produced at their origin and during their subsequent history. The obvious implication of this, ignored in the conventional scientific literature, is that if the radioisotopic ratios do not provide “age” information on recent lava flows because they instead represent fundamental geochemical signatures of the mantle and crustal sources, then the radioisotopic ratios in ancient lava flows also cannot be relied upon to give valid “age” information, because they too are the products of the sources and history of the mantle and crustal rocks that produced them.

This conclusion does not deny the occurrence of radioisotopic decay in rocks and minerals within the geologic record, because there is physical evidence of that decay occurring (such as mature  $^{238}\text{U}$  and  $^{232}\text{Th}$  radiohalos in granitic rocks [62]). It has been suggested that such radioisotopic decay must have occurred at an accelerated rate during distinct events in the earth’s history, such as during the early part of the Creation Week and during the Flood [45]. Such accelerated decay would have left the mantle and crustal sources of magmas with radioisotopic signatures that now yield apparent “ages” in conventional terms representing millions and billions of years of nuclear decay at today’s rates, thus endowing both recent and ancient lava flows with meaningless radioisotopic “ages”, except perhaps in a relative sense within the Biblical framework for the earth’s true history.

Furthermore, if radioisotopic decay was accelerated during the Flood, the resultant accelerated generation of heat is likely to have powered the acceleration of other geologic processes, such as the processes associated with plate tectonics. These would have been responsible during the Flood for catastrophically subducting the pre-Flood ocean floor [2], and mixing mantle and crustal rocks and their radioisotopic contents. At the close of the Flood these plate tectonic processes would have decelerated to their current almost imperceptible rates, but the tectonic framework for the development of the Taupo Volcanic Zone of New Zealand’s North Island would have been put in place. Geophysical investigations indicate that the Pacific Plate today continues to be obliquely subducted beneath the Australian Plate, on which most of New Zealand’s North Island sits. The volcanoes of the Taupo Volcanic Zone, including Ngauruhoe and Ruapehu in the Tongariro Volcanic Center, are about 80 km directly above the subducting Pacific Plate. A zone of earthquakes reveals where the movement is still taking place [69]. Partial melting in the mantle wedge adjacent to the interface with the subducting slab provides a melt with inherited radioisotopic ratios that rises through the mantle wedge from below 80 km depth in the melt column (Figure 9). The melt then ascends through fractures and conduits in the crust above, which is probably less than 20km thick [32], to slowly replenish magma chambers that have in recent decades occasionally erupted to extrude the andesite lava flows. This combination of processes confirms that the radioisotopic ratios in recent lavas are fundamental geochemical characteristics of these rocks, and have no age significance. It is a reasonable general implication that radioisotopic ratios must be among the fundamental geochemical characteristics of ancient lava flows also, reflecting their origin and history rather than indicating valid “ages”.

## CONCLUSIONS

The Rb-Sr, Sm-Nd and Pb-Pb radioisotopic ratios in these samples of the recent (1949–1975) andesite lava flows at Mt Ngauruhoe, New Zealand, as anticipated, do not yield any meaningful “age” information, even with selective manipulation of the data. Instead, these data provide evidence of the mantle source of the lavas, of magma genesis, and of crustal contamination of the parental basalt magmas. Subduction of the Pacific Plate beneath the Taupo Volcanic Arc has carried trench sediments with it — sediments identical in composition to the Torlesse metasediment basement underlying, and outcropping adjacent to, these volcanoes. Scraped off the subducting slab, the sediments have contaminated the basalt magmas generated by partial melting of the peridotitic mantle wedge at the mantle-slab interface. The resultant andesite magmas rose in the melt column through the mantle wedge, and then ascended through fracture conduits in the overlying crust into magma chambers below the volcanoes that erupted when full.

The Sr-Nd-Pb radioisotopic systematics are thus characteristic of the depleted mantle source, modified by mixing with the crustal contaminant. Variations in the depleted mantle Nd “model ages”, which range from 724.5 to 1453.3 Ma, and which are meaningless in this recent (even in conventional terms) tectonic and petrogenetic framework, and the Pb isotopic linear arrays, indicate geochemical heterogeneity in the mantle wedge. Thus the radioisotopic ratios in these recent Ngauruhoe andesite lava flows were inherited from both the peridotitic mantle wedge and the subducted trench sediments, and are fundamental characteristics of their geochemistry. They therefore only reflect the origin and history of the



mantle and crustal sources from which the magma was generated, and therefore have no age significance.

By implication, the radioisotopic ratios in ancient lavas found throughout the geologic record are likely fundamental characteristics of their geochemistry. They therefore probably only reflect the magmatic origin of the lavas from mantle and crustal sources, and any history of mixing or contamination in their petrogenesis, rather than any valid age information. Even though radioisotopic decay has undoubtedly occurred during the earth's history, conventional radioisotopic dating of these rocks therefore does not necessarily provide valid absolute "ages" for them. This is especially so if accelerated nuclear decay accompanied the catastrophic operation of those geologic and tectonic processes responsible for the mixing of the radioisotopic decay products during magma genesis.

## ACKNOWLEDGMENTS

The initiation of this research at Mt Ngauruhoe, New Zealand, was made possible by the logistical support of Answers in Genesis (Australia), who funded both the sample collection and the whole-rock geochemical analyses. The subsequent continuing support for this research by the Institute for Creation Research is gratefully acknowledged — particularly its funding of the significant cost of the Rb-Sr, Sm-Nd and Pb-Pb radioisotopic analyses as part of the RATE (Radioisotopes and the Age of The Earth) project.

## REFERENCES

- [1] Aoki, K. and Fujimaki, H., **Petrology and Geochemistry of Calc-Alkaline Andesite of Presumed Upper Mantle Origin from Itinome-gata, Japan**, American Mineralogist, 67 (1982), pp. 1-13.
- [2] Austin, S.A., Baumgardner, J.R., Humphreys, D.R., Snelling, A.A., Vardiman, L. and Wise, K.P., **Catastrophic Plate Tectonics: A Global Flood Model of Earth History**, Proceedings of the Third International Conference on Creationism, R.E. Walsh, Editor, 1994, Creation Science Fellowship, Pittsburgh, PA, pp. 609-621.
- [3] Battey, M.H., **The Recent Eruption of Ngauruhoe**, Records of the Auckland Institute and Museum, 3(1949), pp. 389-395.
- [4] Bowen, N.L., The Evolution of Igneous Rocks, 1928, Princeton University Press, Princeton, NJ.
- [5] Carter, L., Carter, R.M., McCave, I.N. and Gamble, J.A., **Regional Sediment Recycling in the Abyssal S.W. Pacific Ocean**, Geology, 24 (1996), pp. 735-738.
- [6] Clark, R.H., **Petrology of the Volcanic Rocks of Tongariro Subdivision**, The Geology of the Tongariro Subdivision, D.R. Gregg, New Zealand Geological Survey Bulletin, n.s. 40(1960), pp. 107-123.
- [7] Cole, J.W., **Andesites of the Tongariro Volcanic Centre, North Island New Zealand**, Journal of Volcanology and Geothermal Research, 3(1978), pp. 121-153.
- [8] Cole, J.W., **Structure, Petrology, and Genesis of Cenozoic Volcanism, Taupo Volcanic Zone, New Zealand — A Review**, New Zealand Journal of Geology and Geophysics, 22:6(1979), pp. 631-657.
- [9] Cole, J.W., **Structural Control and Origin of Volcanism in the Taupo Volcanic Zone, New Zealand**, Bulletin of Volcanology, 52 (1990), pp. 445-459.
- [10] Cole, J.W. and Lewis, K.B., **Evolution of the Taupo-Hikurangi Subduction System**, Tectonophysics, 72(1981), pp. 1-21.
- [11] Cole, J.W., Cashman, K.V. and Rankin, P.C., **Rare-Earth Element Geochemistry and the Origin of Andesites and Basalts of the Taupo Volcanic Zone, New Zealand**, Chemical Geology, 38(1983), pp. 255-274.
- [12] Cole, J.W., Graham, I.J., Hackett, W.R. and Houghton, B.F., **Volcanology and Petrology of the Quaternary Composite Volcanoes of Tongariro Volcanic Centre, Taupo Volcanic Zone**, Late Cenozoic Volcanism in New Zealand, I.E.M. Smith, Editor, Royal Society of New Zealand Bulletin, 23(1986), pp. 224-250.
- [13] Conrad, W.K., Nicholls, I.A. and Wall, V.J., **Water-Saturated and Undersaturated Melting of Metaluminous and Peraluminous Crystal Composition at 10kb: Evidence for the Origin of Silicic Magmas in the Taupo Volcanic Zone, New Zealand, and Other Occurrences**, Journal of Petrology, 29 (1988), pp. 765-803.



- [14] Davidson, J., **Mechanisms of Contamination in Lesser Antilles Island Arc Magmas from Radiogenic and Oxygen Isotope Relationships**, Earth and Planetary Science Letters, 72 (1985), pp. 163-174.
- [15] Davies, J.H. and Stevenson, D.J., **Physical Model of Source Region of Subduction Zone Volcanics**, Journal of Geophysical Research, 97 (1992), pp. 2037-2070.
- [16] DePaolo, D.J., **Trace Element and Isotopic Effects of Combined Wallrock Assimilation and Fractional Crystallisation**, Earth and Planetary Science Letters, 53 (1981), pp. 189-202.
- [17] DePaolo, D.J. and Wasserburg, G.J., **Nd Isotopic Variations and Petrogenetic Models**, Geophysical Research Letters, 3 (1976), pp. 249-252.
- [18] Dicken, A.P., Radiogenic Isotope Geology, 1995, Cambridge University Press, Cambridge, England.
- [19] Ewart, A., **Notes of the Chemistry of Ferromagnesian Phenocrysts of Selected Volcanic Rocks, Central Volcanic Region**, New Zealand Journal of Geology and Geophysics, 14:2 (1971), pp. 323-340.
- [20] Ewart, A. and Stipp, J.J., **Petrogenesis of the Volcanic Rocks of the Central North Island, New Zealand, as Indicated by a Study of Sr<sup>87</sup>/Sr<sup>86</sup> Ratios, and Sr, Rb, K, U and Th Abundances**, Geochimica et Cosmochimica Acta, 32(1968), pp. 699-736.
- [21] Ewart, A. and Hawkesworth, C.J., **The Pleistocene to Recent Tonga-Kermadec Arc Lavas: Interpretation of New Isotope and Rare Earth Data in Terms of a Depleted Source Model**, Journal of Petrology, 28 (1987), pp. 495-530.
- [22] Faure, G., Principles of Isotope Geology, second edition, 1986, John Wiley and Sons, New York.
- [23] Francis, P.W., Thorpe, R.S., Moorbath, S., Kretzschmar, G.A. and Hammill, M., **Strontium Isotope Evidence for Crustal Contamination of Calc-Alkaline Volcanic Rocks from Cerro Galan, Northwest Argentina**, Earth and Planetary Science Letters, 48 (1980), pp. 257-267.
- [24] Gamble, J.A., Smith, I.E.M., Graham, I.J., Kokelaar, B.J., Cole, J.W., Houghton, B.F. and Wilson, C.J.N., **The Petrology, Phase Relations and Tectonic Setting of Basalts from the Taupo Volcanic Zone New Zealand and the Kermadec Island Arc – Havre Trough, S.W. Pacific**, Journal of Volcanology and Geothermal Research, 43 (1990), pp. 235-270.
- [25] Gamble, J.A., Smith, I.E.M., McCulloch, M.T., Graham, I.J., and Kokelaar, B.P., **The Geochemistry and Petrogenesis of Basalts from the Taupo Volcanic Zone and Kermadec Island Arc, S.W. Pacific**, Journal of Volcanology and Geothermal Research, 54 (1993), pp. 265-290.
- [26] Gamble, J.A., Woodhead, J.D., Wright, I. and Smith, I., **Basalt and Sediment Geochemistry and Magma Petrogenesis in a Transect from Ocean Island Arc to Rifted Continental Margin Arc: The Kermadec-Hikurangi Margin, SW Pacific**, Journal of Petrology, 37:6 (1996), pp. 1523-1546.
- [27] Gamble, J.A., Wood, C.P., Price, R.C., Smith, I.E.M., Stewart, R.B. and Waight, T., **A Fifty Year Perspective of Magmatic Evolution on Ruapehu Volcano, New Zealand: Verification of Open System Behaviour in an Arc Volcano**, Earth and Planetary Science Letters, 170(1999), pp. 301-314.
- [28] Gill, J.B., Orogenic Andesites and Plate Tectonics, 1981, Springer-Verlag, Berlin.
- [29] Graham, I.J., **Rb-Sr Geochronology and Geochemistry of Torlesse Metasediments from the Central North Island, New Zealand**, Chemical Geology, 52 (1985), pp. 317-331.
- [30] Graham, I.J., Petrochemical and Sr Isotopic Studies of the Lavas and Xenoliths from Tongariro Volcanic Centre — Implications for Crustal Contamination in Calc-Alkaline Magmas, Ph.D. Thesis (unpublished), Victoria University of Wellington (1985).
- [31] Graham, I.J., **Petrography and Origin of Metasedimentary Xenoliths in Lavas from Tongariro Volcanic Center**, New Zealand Journal of Geology and Geophysics, 30 (1987), pp. 139-157.
- [32] Graham, I.J. and Hackett, W.R., **Petrology of Calc-Alkaline Lavas from Ruapehu Volcano and Related Vents, Taupo Volcanic Zone, New Zealand**, Journal of Petrology, 28:3(1987), pp. 531-567.
- [33] Graham, I.J., Grapes, R.H. and Kifle, K., **Buchitic Metagreywacke Xenoliths from Mount Ngauruhoe, Taupo Volcanic Zone, New Zealand**, Journal of Volcanology and Geothermal

- Research, 35 (1988), pp. 205-216.
- [34] Graham, I.J. and Cole, J.W., **Petrogenesis of Andesites and Dacites of White Island Volcano, Bay of Plenty, New Zealand in the Light of New Geochemical and Isotopic Data**, New Zealand Journal of Geology and Geophysics, 34 (1991), pp. 303-315.
- [35] Graham, I.J., Gulson, B.L., Hedenquist, J.W. and Mizon, K., **Petrogenesis of Late Cenozoic Volcanic Rocks from the Taupo Volcanic Zone, New Zealand, in the Light of New Pb Isotope Data**, Geochimica et Cosmochimica Acta, 56 (1992), pp. 2797-2819.
- [36] Graham, I.J., Cole, J.W., Briggs, R.M., Gamble, J.A. and Smith, I.E.M., **Petrology and Petrogenesis of Volcanic Rocks from the Taupo Volcanic Zone: A Review**, Journal of Volcanology and Geothermal Research, 68(1995), pp. 59-87.
- [37] Gregg, D.R., **Eruption of Ngauruhoe 1954-55**, New Zealand Journal of Science and Technology, B37(1956), pp. 675-688.
- [38] Gregg, D.R., **The Geology of Tongariro Subdivision**, New Zealand Geological Survey Bulletin, n.s. 40(1960).
- [39] Grindley, G.W., Geological Map of New Zealand 1:250,000 Sheet 8 — Taupo, New Zealand Geological Survey (1960).
- [40] Grindley, G.W., **Tongariro National Park, Stratigraphy and Structure**, New Zealand Department of Scientific and Industrial Research Information Series, 50(1965), pp. 79-86.
- [41] Hackett, W.R. and Houghton, B.F., **Active Composite Volcanoes of Taupo Volcanic Zone, Central North Island Volcanism**, New Zealand Geological Survey Record 21(1987), pp. 61-114.
- [42] Hackett, W.R. and Houghton, B.F., **A Facies Model for a Quaternary Andesitic Composite Volcano: Ruapehu, New Zealand**, Bulletin of Volcanology, 51 (1989), pp. 51-68.
- [43] Hart, S.R., **The DUPAL Anomaly: A Large-Scale Isotopic Anomaly in the Southern Hemisphere**, Nature, 309 (1984), pp. 753-756.
- [44] Hofmann, A.W. and Hart, S.R., **An Assessment of Local and Regional Isotopic Equilibrium in the Mantle**, Earth and Planetary Science Letters, 38 (1978), pp. 44-62.
- [45] Humphreys, D.R., **Accelerated Nuclear Decay: A Viable Hypothesis?**, Radioisotopes and the Age of the Earth: A Young-Earth Creationist Research Initiative, L. Vardiman, A.A. Snelling and E.F. Chaffin, Editors, 2000, Institute for Creation Research, El Cajon, CA and Creation Research Society, St. Joseph, MO, pp. 333-379.
- [46] Ito, E., White, W.M. and Gopel, C., **The O, Sr, Nd and Pb Isotope Geochemistry of MORB**, Chemical Geology, 62 (1987), pp. 157-176.
- [47] James, D.E., **The Combined Use of Oxygen and Radiogenic Isotopes as Indicators of Crustal Contamination**, Annual Review of Earth and Planetary Sciences, 9 (1981), pp. 311-344.
- [48] Kushiro, I., **Melting of Hydrous Upper Mantle and Possible Generation of Andesitic Magma: An Approach from Synthetic Systems**, Earth and Planetary Science Letters, 22 (1974), pp. 294-299.
- [49] McCulloch, M.T. and Perfit, M.R.,  **$^{143}\text{Nd}/^{144}\text{Nd}$ ,  $^{87}\text{Sr}/^{86}\text{Sr}$  and Trace Element Constraints on the Petrogenesis of Aleutian Island Arc Magmas**, Earth and Planetary Science Letters, 56 (1981), pp. 167-179.
- [50] McCulloch, M.T. and Black, L.P., **Sm-Nd Isotopic Systematics of Enderby Land Granulites and Evidence for the Redistribution of Sm and Nd during Metamorphism**, Earth and Planetary Science Letters, 71 (1984), pp. 46-48.
- [51] McCulloch, M.T., Kyser, T.K., Woodhead, J.D. and Kinsley, L., **Pb-Sr-Nd-O Isotopic Constraints on the Origin of Rhyolites from the Taupo Volcanic Zone of New Zealand: Evidence for Assimilation followed by Fractionation of Basalt**, Contributions to Mineralogy and Petrology, 115 (1994), pp. 303-312.
- [52] Mortimer, N. and Parkinson, D., **Hikurangi Plateau: A Cretaceous Large Igneous Province in the Southwest Pacific Ocean**, Journal of Geophysical Research, 101 (1996), pp. 687-696.
- [53] Mysen, B.O. and Boettcher, A.L., **Melting of a Hydrous Mantle, II. Geochemistry of Crystals and Liquids formed by Anatexis of Mantle Peridotite at High Pressures and High Temperatures as a function of controlled activities of Water, Hydrogen and Carbon Dioxide**,

- Journal of Petrology, 16 (1975), pp. 549-593.
- [54] Nairn, I.A., **Atmospheric Shock Waves and Condensation Clouds from Ngauruhoe Explosive Eruptions**, Nature, 259 (1976), pp. 190-192.
- [55] Nairn, I.A. and Self, S., **Explosive Eruptions and Pyroclastic Avalanches from Ngauruhoe in February 1975**, Journal of Volcanology and Geothermal Research, 3(1978), pp. 39-60.
- [56] Nairn, I.A. and Wood, C.P., **Active Volcanoes and Geothermal Systems, Taupo Volcanic Zone**, New Zealand Geological Survey Record 22 (1987), pp. 5-84.
- [57] Nairn, I.A., Hewson, C.A.Y., Latter, J.H. and Wood, C.P., **Pyroclastic Eruptions of Ngauruhoe Volcano, Central North Island, New Zealand, 1974 January and March**, Volcanism in Australasia, R.W. Johnson, Editor, 1976, Elsevier, Amsterdam, pp. 385-405.
- [58] Nohda, A., **Classification of Island Arcs by Nd-Sr Isotopic Data**, Geochemical Journal, 18 (1984), pp. 1-9.
- [59] Rollinson, H., Using Geochemical Data: Evaluation, Presentation, Interpretation, 1993, Addison Wesley Longman, Harlow, England.
- [60] Snelling, A.A., **The Cause of Anomalous Potassium-Argon "Ages" for Recent Andesite Flows at Mt Ngauruhoe, New Zealand, and the Implications for Potassium-Argon "Dating"**, Proceedings of the Fourth International Conference on Creationism, R.E. Walsh, Editor, 1998, Creation Science Fellowship, Pittsburgh, PA, pp. 503-525.
- [61] Snelling, A.A., **Geochemical Processes in the Mantle and Crust**, Radioisotopes and the Age of the Earth: A Young-Earth Creationist Research Initiative, L. Vardiman, A.A. Snelling and E.F. Chaffin, Editors, 2000, Institute for Creation Research, El Cajon, CA, and Creation Research Society, St. Joseph, MO, pp. 123-304.
- [62] Snelling, A.A. and Armitage, M.H., **Radiohalos — A Tale of Three Granitic Plutons**, Proceedings of the Fifth International Conference on Creationism, 2003, Creation Science Fellowship, Pittsburgh, PA, this volume.
- [63] Steiner, A., **Petrogenetic Implications of the 1954 Ngauruhoe Lava and Its Xenoliths**, New Zealand Journal of Geology and Geophysics, 1(1958), pp. 325-363.
- [64] Stipp, J.J., The Geochronology and Petrogenesis of the Cenozoic Volcanics of the North Island, New Zealand, Ph.D. Thesis (unpublished), Australian National University, Canberra (1968).
- [65] Tatsumi, Y., **Formation of the Volcanic Front in Subduction Zones**, Geophysical Research Letters, 13 (1986), pp. 717-720.
- [66] Taylor, H.P., **The Effects of Assimilation of Country Rocks by Magmas on  $^{18}\text{O}/^{16}\text{O}$  and  $^{87}\text{Sr}/^{86}\text{Sr}$  Systematics in Igneous Rocks**, Earth and Planetary Science Letters, 47 (1980), pp. 243-253.
- [67] Taylor, S.R. and McLennan, S.M., The Continental Crust: Its Composition and Evolution, 1985, Blackwell, Oxford, England.
- [68] Topping, W.W., **Tephrostratigraphy and Chronology of Late Quaternary Eruptives from the Tongariro Volcanic Centre, New Zealand**, New Zealand Journal of Geology and Geophysics, 16(1973), pp. 397-423.
- [69] Williams, K., Volcanoes of the South Wind: A Field Guide to the Volcanoes and Landscape of the Tongariro National Park, 1994, Tongariro Natural History Society, Tuarangi, New Zealand.
- [70] Wilson, C.J.N., Houghton, B.F., McWilliams, M.O., Lanphere, M.A., Weaver, S.D. and Briggs, R.M., **Volcanic and Structural Evolution of Taupo Volcanic Zone, New Zealand: A Review**, Journal of Volcanology and Geothermal Research, 68 (1995), pp. 1-28.
- [71] Wyllie, P.J., **Constraints Imposed by Experimental Petrology on Possible and Impossible Magma Sources and Products**, Philosophical Transactions of the Royal Society of London, Series A, 310 (1984), pp. 439-456.